coatings

MDPI

Review

Nanomaterials for Potential Detection and Remediation: A Review of Their Analytical and Environmental Applications

Sebastián Salazar Sandoval [1,†], Tamara Bruna [2,*,†], Francisca Maldonado-Bravo [1], Paul Jara [1], Nelson Caro [2], Carlos Rojas-Romo [1], Jorge González-Casanova [3], Diana Rojas Gómez [4], Nicolás Yutronic [1], Marcela Urzúa [1] and Annia Rodríguez-San Pedro [5,*]

[1] Departamento de Química, Facultad de Ciencias, Universidad de Chile, Las Palmeras 3425, Ñuñoa, Santiago 7800003, Chile; sebasalazar@ug.uchile.cl (S.S.S.); francisca.maldonado@ug.uchile.cl (F.M.-B.); pjara@uchile.cl (P.J.); carlosrojas@uchile.cl (C.R.-R.); nyutroni@uchile.cl (N.Y.); maurzua@uchile.cl (M.U.)
[2] Centro de Investigación Austral Biotech, Facultad de Ciencias, Universidad Santo Tomás, Avenida Ejército 146, Santiago 8320000, Chile; nelsoncarofu@santotomas.cl
[3] Facultad de Ciencias de la Salud, Instituto de Ciencias Biomédicas, Universidad Autónoma de Chile, Santiago 8910060, Chile; jorge.gonzalez@uautonoma.cl
[4] Escuela de Nutrición y Dietética, Facultad de Medicina, Universidad Andrés Bello, Santiago 8370321, Chile; diana.rojas@unab.cl
[5] Centro de Investigación e Innovación Para el Cambio Climático (CiiCC), Facultad de Ciencias, Universidad Santo Tomás, Avenida Ejército 146, Santiago 8320000, Chile
* Correspondence: tbruna@santotomas.cl (T.B.); arodriguezs@santotomas.cl (A.R.-S.P.)
† Main authors.

Abstract: The rapid increase in industrialization and human population is leading to critical levels of environmental pollutants, such as agrochemicals or heavy metals, which affect the preservation and integrity of ecosystems, the accessibility to drinking water sources, and the quality of the air. As such, remediation of these issues demands strategies for implementing and designing novel technologies. In that regard, nanomaterials have unique physicochemical properties that make them desirable candidates for the detection and remediation of environmental pollutants. The scope of this review is to provide an analysis of the available nanomaterials that are being used as an approach to detect and remediate hazardous residues, comprising systems such as noble metals, biosensors, cyclodextrin-based polymers, and graphene oxide nanocomposites, to name a few. Furthermore, this work discusses said nanomaterials in terms of their effectiveness, sustainability, and selectivity as a guideline for researchers wishing to indulge in this relevant study area.

Keywords: nanocomposites; nanoparticles; enzyme-loaded nanoparticles; cyclodextrin nanosponges; water remediation; air detection; heavy metals; agrochemicals; selectivity; reproducibility

Citation: Salazar Sandoval, S.; Bruna, T.; Maldonado-Bravo, F.; Jara, P.; Caro, N.; Rojas-Romo, C.; González-Casanova, J.; Gómez, D.R.; Yutronic, N.; Urzúa, M.; et al. Nanomaterials for Potential Detection and Remediation: A Review of Their Analytical and Environmental Applications. *Coatings* **2023**, *13*, 2085. https://doi.org/10.3390/coatings13122085

Academic Editor: Gianfranco Carotenuto

Received: 9 November 2023
Revised: 7 December 2023
Accepted: 11 December 2023
Published: 14 December 2023

1. Introduction

Considering the current climate crisis and the progress of the industries that continue to grow each year, the ability to detect analytes, polluting, and potentially toxic products for the environment and human beings has taken on greater relevance. The early and optimal detection of substances accumulating in ecosystems allows for the taking of measures to remedy or reduce the presence of these substances in the environment. The substances of significant interest are chemical residues such as agrochemicals and their derivates and heavy metals [1,2]. Each principal feature is their long-term persistence in the environment because they react and interact with substances present in it and bioaccumulate. The detection of pollutants or chemicals in media is carried out by taking samples from the area of interest, be it an ecosystem, industrial waste ponds, natural water sources, or water intended for human consumption. Subsequently, the samples are analyzed using different advanced laboratory technologies, such as inductively coupled plasma mass spectrometry/atomic emission spectrometer, atomic absorption spectrometry, atomic fluorescence

spectrometry, and laser-induced breakdown spectrometry, which, despite having high capacity and precision, require high consumption of time and energy and are difficult to perform [3].

The development of sensors or devices capable of detecting these pollutants has increasingly become a viable alternative to replace or accompany the classical techniques used for detection. Sensor manufacturing is focused on improving characteristics such as specificity, detection limits, and detection time [4,5]. The development of new materials has made it possible to generate transportable, manipulable, and stable sensors.

Nanotechnology has provided us with a platform with various applications to increase a sustainable environment for present generations and thus be able to carry out future research. Nanomaterials have been incorporated into these lines of study and have proven highly compatible with applications in contaminants and toxic chemical detection from natural environments [6,7]. In general, materials on the nanometric scale have optical, electrical, and mechanical properties that are not observable on the macro (or bulk) scale [8,9], allowing the creation of sensors with faster detection, better specificity, catalysis, and better quality of the transduction signal. Further, as nanomaterials present a high ratio of their surface-area-to-volume ratio, they are also appropriate for wastewater remediation processes [10]. This review discusses the importance of various nanomaterials for detecting and remediating pollutants as an alternative to traditional methods, considering the sustainability of such materials, their ability to be reused or recycled, and their specificity towards the target analytes. In that regard, our motivation to write this review resides in the potential applicability of nanomaterials to overcome the pollution crisis in the foreseeable future. However, despite their enormous potential, nanomaterials also present a fair number of challenges, which will also be addressed in this review to provide insight and strategies for researchers who might indulge in pollutant treatment using nanostructures. Finally, the remediation and detection of pollutants using nanotechnology will be discussed in three categories, as described in Figure 1.

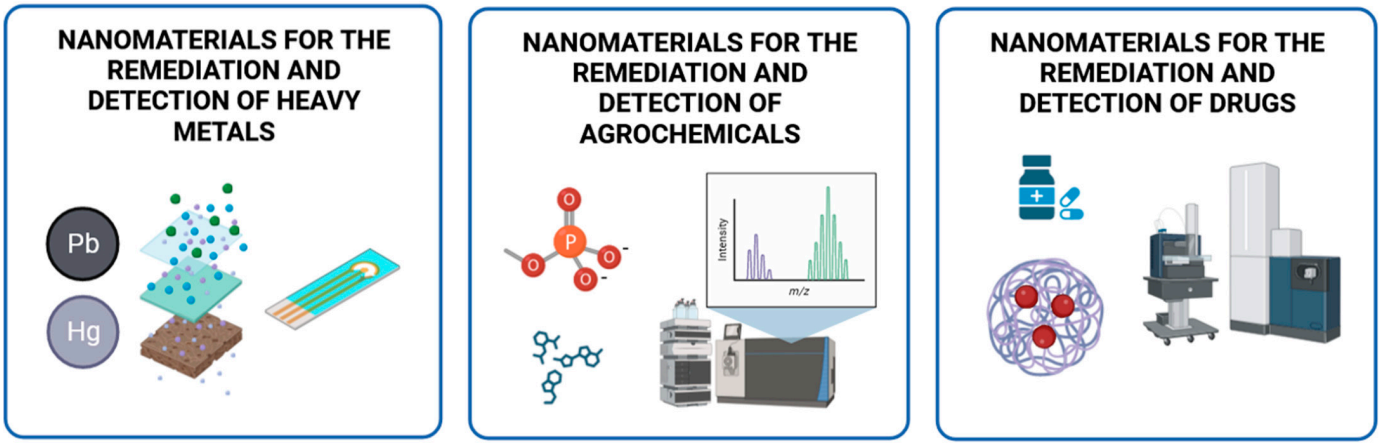

Figure 1. Nanomaterials and their application in the detection and removal of pollutants. Created with BioRender.com.

2. Nanomaterials for the Detection of Heavy Metals

Due to the high industrial activity, the associated residues and wastes are constantly increasing and accumulating in surrounding soils and wastewater. Notably, heavy metals have raised concerns due to their toxic nature and the resulting consequences for the environment and human health, even at low concentrations. Heavy metals such as arsenic, cadmium, chromium, lead, and mercury are relevant in this context due to their deposition by industrial activities and their well-known high degree of toxicity. They are considered systemic toxicants capable of inducing damage to multiple organs, even at lower levels of exposure. Therefore, it is essential to detect them even at low concentrations [11,12].

Industries and governments employ various techniques to detect ions and trace levels of these elements in different substrates.

These techniques commonly involve absorption spectroscopy, inductively coupled plasma atomic emission spectroscopy, optical emission spectroscopy, fluorescence spectroscopy, and other methods. While these methods are highly adaptable and versatile, enabling simultaneous analysis of multiple elements, they also have certain drawbacks.

These disadvantages include the need for specialized equipment, high energy consumption, the requirement for sample preparation steps, and longer analysis times [3].

Nanotechnology provides new nanomaterials and nanoparticles (NPs) that can be applied in the field of remediation of heavy metals [13]. These include noble metal NPs, carbon-based nanomaterials, oxide NPs, and nanocomposites. The versatility of nanomaterials lies in the various forms and structures that can be obtained using different synthesis methods, resulting in a wide range of morphologies with unique optical, catalytic, and electrical properties [14].

2.1. Noble Metal NPs for the Colorimetric Detection of Heavy Metals

Given the large number of heavy metals deposited in the environment, the fast and simple detection of these metals has become a matter of concern. Accessible and easy sensing of heavy metals enables constant monitoring of their levels in ecosystems and contributes to tracing the deposition and migration of these materials in the environment and substrates [15,16].

Related to this, metallic nanostructures exhibit several properties that make them suitable for pollutant detection. Incorporation into sensing devices can improve not only the detection capacity of the sensors but also facilitate the transduction of the signal derived from the sensing. The principal elements studied for these applications are gold, silver, zinc, and titanium [17–20]. Specifically, silver (AgNPs), copper (CuNPs), and gold (AuNPs) nanoparticles are the most investigated for their use in remediation and sensing applications. The properties that these metals have at a nanometric scale are related to their disposition and structure. Thus, the surface plasmon resonance (SPR) phenomena, which is characteristic of nanosilver and nanogold structures, has been employed for the development of colorimetric sensors.

Colorimetric sensors are systems that exhibit a color change upon detecting the molecule of interest; this change can be easily detected by the naked eye or, more specifically, by UV spectrophotometry. Nanomaterials based on gold and silver are the most exploited for these applications since different concentrations of the analyte of interest can cause nanomaterials to aggregate, precipitate, or change their structure. These alterations in the original state of the nanomaterials will induce a related change in the SPR [21,22].

In addition to using nanomaterials as sensors, these have been incorporated into structures to develop more sophisticated devices, allowing them to increase their detection capacity and signal transduction, among other sensor properties [23].

As mentioned, the most straightforward kind of sensor investigated in this area are the colorimetric sensors, which allow easy and rapid detection that can be applied even to detect metallic contaminants in the environment. An example of this is the colorimetric assay developed by Dong et al. [24] using chalcone carboxylic acid-capped AgNPs for the specific detection of Cd (II). In this case, the capping agent primarily provided the functional group (OH) with which Cd^{2+} ions interact, leading to a complex formation.

The interaction between Cd (II) and the carboxylic acid eventually induces AgNPs aggregation, which can be easily detected because of the color change of the solution and by changes in the plasmonic absorbance peak of the AgNPs solution. These changes were directly related to Cd (II) concentration. As reported by these authors, the same effect was not induced by other metallic ions that could be present in environmental samples.

Systems based on changes in the SPR of AgNPs have also been designed for sensing other contaminant ions. Generally, in these systems, the functionalization or capping of the NPs determines their detection ability and selectivity. Molecules with thiol groups have

been explored as capping agents in the synthesis of AgNPs, as it is known they bind to the nanoparticle's surface by Ag—S bonds stabilizing the NPs [25].

Thus, the selected agent to functionalize NPs is imperative for achieving good reactivity and specificity in analytes. Related to this, Rossi et al. [26] used mercaptoundecanoic acid (11 MUA) to synthesize 11 MUA—functionalized AgNPs used in solution as a colorimetric sensor for detecting Ni (II). Only when the AgNPs-11 MUA were used for Ni^{2+} ion detection changes in the absorption band characteristic for AgNPs (near 420 nm) and the appearance of a second absorption band at 477 nm were observed.

These two bands' appearance was directly related to the concentration of Ni^{2+} ions added, and the limit of detection (LOD) achieved was 2.15 μM.

AgNPs showed the ability to detect Ni (II) and Co (II) in a study where these NPs were capped with (3-mercaptopropyl) trimethoxy silane (3 MPS). The assay developed in this work showed that AgNPs—3 MPS could detect nickel and cobalt ions with a sensitivity limit of 500 ppb for both elements. The detection mechanism is based on the formation of coordination compounds of Ni (II) and Co (II) with the AgNPs. As it could be detected, the addition of these ions induced changes in the ζ-potential of NPs, which supports the effective interaction between Ni (II) and Co (II) with the AgNPs—3MPS and subsequent aggregation of the NPs induced by the formation of the coordination compounds. As expected, because of the changes in the dispersity and size of NPs, the presence of these ions in the solution was reflected in changes in the SPR [27].

In a similar study, AgNPs stabilized with the same ligand (3 MPS) were tested to interact with Hg (II) for potential sensing applications [28]. The study probed that in the presence of Hg^{2+}. These ions would uniformly distribute on the surface of the NPs, forming an Ag/Hg amalgam that caused changes in the SPR spectra and, therefore, in the color of the solution tested.

Because of their optical, chemical, and catalytic properties, as well as being cost-effective compared to other elements, AgNPs have been studied, as mentioned, for the detection of Hg (II). AgNPs functionalized with 2-aminopyrimidine-4,6-diol (APD) were probed to chelate Hg^{2+} ions. The colorimetric detection of Hg^{2+} ions was achieved and related to a complex formation between APD-AgNPs and Hg (II), which would induce aggregation and a change of the system color from pale brown to bright yellow, given the change in the surface resonance plasmon. The LOD reached was 0.35 μm/L, and the detection time needed was 5 min, even at low concentrations [29].

Similarly, Sharma et al. [30] report a sensing method for Hg^{2+} by using thiol-terminated chitosan as a capping agent during the synthesis of AgNPs. The solutions with these modified Ch-AgNPs were used to detect Hg (II) in drinking water samples, exhibiting good performance and a LOD of 1.7×10^{-8} M. In this study, the colorimetric change was analyzed by transmission electron microscopy (TEM) and dynamic light scattering (DLS), confirming the change in the structure of the NPs induced by the redox interaction between AgNPs and mercury ions. Therefore, this work also reported the separation of Hg^{2+} from water samples by changing the pH of the solutions.

Garg et al. [31] probed that xylenol orange synthesized—AuNPs can be used as an optical sensor of Al (III) based on aggregating these in the presence of the contaminant.

As the characteristic plasmon exhibited by AuNPs is in the visible light region, the color change produced by the aggregation of NPs as they detect the target ion is also visible to the naked eye. The AuNPs could detect Al (III) in water samples with an LOD of 12 ppm.

An ultrasensitive Hg (II) detector was reported by Sadani et al. [32]. The sensor consisted of chitosan-capped AuNPs on bovine serum albumin (BSA) deposited on an optical fiber platform. The interaction of Hg^{2+} with the sensor was attributed to Hg (II)'s strong affinity towards the functional groups in chitosan and BSA. Further, an increase in the absorbance of the SPR of AuNPs was observed. Colorimetric detection of Hg^{2+} was tested on actual samples, such as tap, sewage, or marine water. The determined LODs were 0.1 ppb in tap water and 0.2 ppb in seawater, with high selectivity towards mercury.

Likewise, Yuan et al. [33] developed an optic sensor based on 4-mercaptopyridine (4-MPY) modified AuNPs assembled on an Au surface for Hg(II) detection. The exposed pyridinic nitrogen of 4-MPY coordinates with the Hg^{2+} ions via multidentate N-bonding to form a Hg-pyridine complex and a coupling effect between Au film and AuNPs, generating strong SPR wavelength shifts that were dependent on Hg^{2+} concentration. The sensor LOD was 8 nM in tap water samples under optimal conditions.

It is worth noting that in all cases, the benefit of the developed methods is that, in addition to detecting ions in small concentrations, the sensing can be detected by the bare eye because of the color change in the solutions containing NPs as the morphological characteristics of these nanomaterials vary. This represents a significant advantage since all the commonly used methods for sensing and/or detection of heavy metals involve sample treatment and expensive instrumentation and are time-consuming [34].

The basic colorimetric sensors can be upgraded using two agents to functionalize the NPs. As demonstrated by a nano-sensor for Ni (II) detection using AgNPs functionalized with sodium dodecyl sulfonate (SDS) and adenosine monophosphate (AMP). Ni^{2+} induced the aggregation of the AMP-SDS-AgNPs by the cooperative effect of the interactions between Ni (II) and each capping agent. This causes a decrease in the plasmon absorbance band near 400 nm of AgNPs and the appearance of a different band near 500 nm, which is related to the concentration of the Ni^{2+} ion. In this case, the sensor exhibited good selectivity and performance in detecting Ni^{2+} in actual water samples, with recoveries in the range of 98.4 to 106%. The LOD achieved with this sensor was 0.6 μM in an aqueous solution. The optimized detection method shows promising potential for being used in Ni (II) detection in actual samples as it exhibited high recovery percentages either in a lake or tap water and as its LOD tested was lower than the allowed in water for these ions in drinking water (45 μM) [35].

Another example is AgNPs functionalized with citric acid and L-cysteine, which exhibit the ability for Hg^{2+} ion sensing and excellent stability in simulated aqueous media as a consequence of the stabilizing agents [36]. The synthesized NPs were used in solution to detect Hg^{2+} ions; the results were that in the presence of Hg (II), a redshift of the SPR of NPs related to their concentration was observed, with an estimated detection limit for this system of 0.6 ppm.

A colorimetric sensor for Hg (II) was developed through the dispersion of silver and copper bimetallic NPs into a SiO_2-TiO_2-ZrO_2 ternary matrix [37]. Hg (II) concentrations were determined by analyzing the variations in the intensity of the SPR bands. The sensor was tested on river and well water, achieving a LOD of 0.1 μM in both samples. Moreover, selectivity was investigated among heavy metals, such as Ni (II), Cd (II), Se (IV), Mn (II), and Zn (II).

The plasmonic phenomena of noble metal NPs depend not only on their size and dispersion but also on their shape, dielectric environment, and interactions with particles nearby [38]. Furthermore, aggregation, shape transformations, and reorder caused in the nanomaterials induced by the presence of determined heavy metals have been extensively explored for the development of colorimetric sensors.

Metallothionein-capped CuNPs (MT-CuNPs) were synthesized for colorimetric detection of Hg (II) and Cd (II) based on catalase-like activity [39]. The method consisted of the visual and spectrophotometric analysis of MT-CuNPs upon the addition of Hg^{2+} and Cd^{2+}. Moreover, TEM micrographs evidenced that both heavy metals induced the aggregation of the MT-CuNPs system, which is consistent with the wavelength shifts of the SPR band.

A study involving Ranolazine-capped CuNPs (R-CuNPs) was conducted by Laghari et al. [40] for a highly sensitive colorimetric sensor of As (III) in water samples. The R-CuNPs system displayed an SPR band at 573 nm, which evidenced reduced adsorption and a bathochromic shift upon the addition of As (III). The presence of As^{3+} ions triggered the release of ranolazine from the CuNPs surface, inducing their aggregation and a color variation from brick red to dark green.

Yoon et al. [41] proposed using silver nano-prisms for sensing Ni (II) in search of an improvement in sensitivity. In the study, the concentration of Ni^{2+} ions were determined by changes in the triangular form of silver nano-prisms in a solution with O_2 and H_2O, in which the addition of Ni (II) would catalyze the formation of an H_2O_2 agent that would induce the etching of the prisms.

This was reflected in a color change from blue to reddish brown and exhibited in a more prominent blue shift of the surface plasmon. The LOD achieved in this system was 21.6 nM under optimal conditions.

A method for Cd (II) detection was proposed by Gan et al. based on aptamer-functionalized AuNPs [42]. The colorimetric detection of Cd^{2+} ions is attained through its interaction with the aptamers, thus weakening the stability of AuNPs and triggering a change of color in the solution. The colorimetric change was analyzed using a smartphone-based colorimetric system, obtaining an LOD of 1.13 μg/L.

Some colorimetric methods for heavy metal detection using noble metal nanoparticles are illustrated in Figure 2.

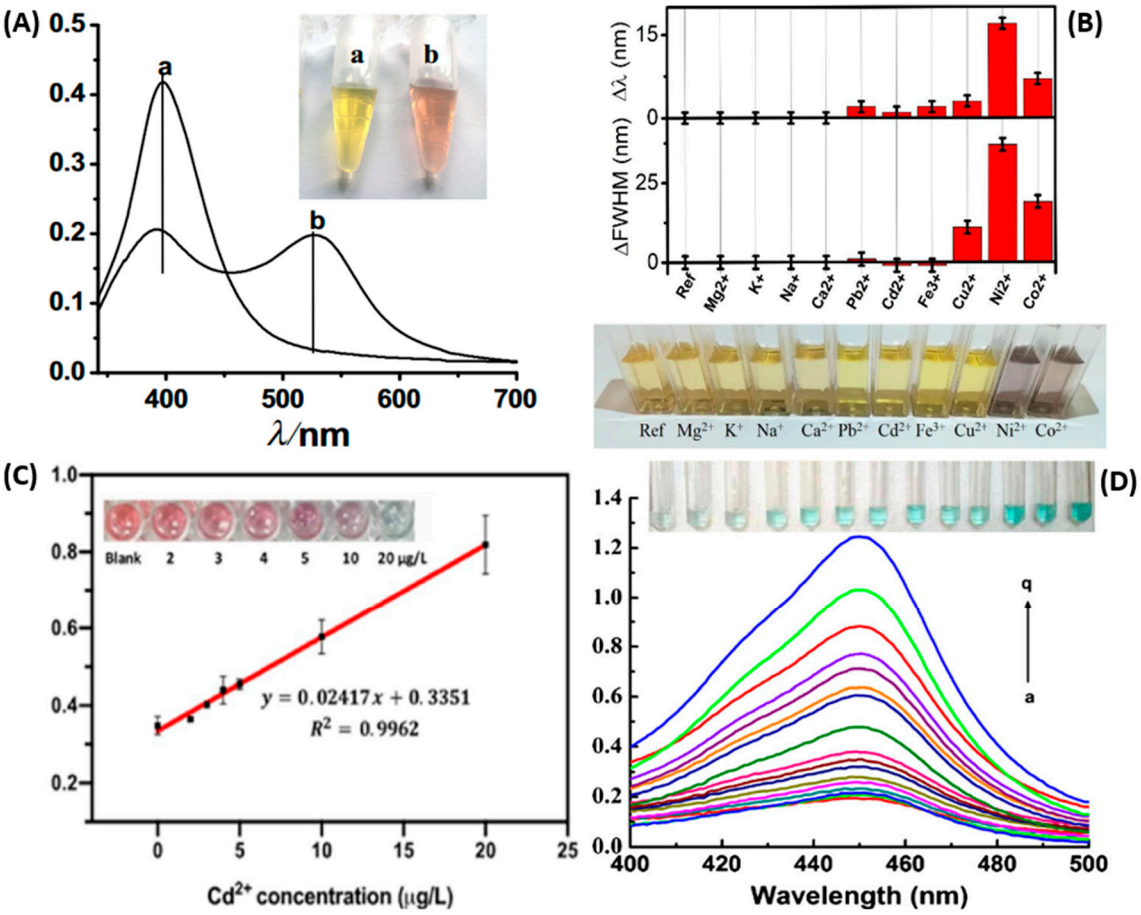

Figure 2. Nanomaterials for the colorimetric detection of heavy metals. The nanomaterial-analyte interaction is confirmed through changes in the state of the nanomaterial: Absorption spectra of the CCA-AgNPs probe before (**a**) and after (**b**) interaction with Cd(II) (**A**) [24]. The colorimetric aspect of 3-MPS-AgNPs upon interaction with different metal ions. Changes in the SPR absorption band and the full width at half maximum (FWHM) are also illustrated (**B**) [27]. Colorimetric response of an aptamer-AuNPs system at increasing Cd (II) concentrations (**C**) [42]. Absorption spectra and colorimetric response of MT-CuNPs (450 nm) at different Pb (II) concentrations (**D**) [39].

The noble metal NPs discussed in this section are summarized in Table 1, along with the heavy metals that were detected.

Table 1. Summary of noble metal NPs and their application as treatments for heavy metals.

System	Heavy Metal	Altered State of the Metal NPs	Polluted Matrix	Reference
Chalcone carboxylic acid-capped AgNPs	Cd (II)	Carboxylic acid-Cd interaction induced AgNPs aggregation	Drinking water and lake water	[24]
11 MUA—functionalized AgNPs	Ni (II)	Red shift in the SPR of AgNPs	Lab water	[26]
3 MPS-AgNPs	Co (II) and Ni (II)	Aggregation of AgNPs induced by the formation of coordination compounds	Lab water	[27]
3 MPS-AgNPs	Hg (II)	Formation of an Ag/Hg amalgam that causes changes in the SPR spectra	Lab water	[28]
APD-AgNPs	Hg (II)	Complex formation between APD-AgNPs and Hg^{2+}, inducing change of the system color	Lab water	[29]
Chitosan-AgNPs	Hg (II)	Change in the structure of AgNPs	Drinking water	[30]
AMP-SDS-AgNPs	Ni (II)	Decrease in the plasmon absorbance band due to the interactions between Ni^{2+} and each capping agent	Tap water and lake water	[35]
L-cysteine-AgNPs	Hg (II)	Red shift of AgNPs SPR band	Salt water and drinking water	[36]
Silver nano prisms	Ni (II)	Changes in the triangular form of silver nano-prisms in a solution with O_2 and H_2O	Tap water and pond water	[41]
Xylenol orange-AuNPs	Al (III)	Aggregation and color change of AuNPs	Drinking water	[31]
Chitosan-BSA-AuNPs	Hg (II)	Hg (II) strong affinity towards chitosan and BSA promoted changes in the SPR of AuNPs	Water, soil, and food samples	[32]
4-MPY-AuNPs	Hg (II)	Hg-pyridine complex formation and a coupling effect between Au film and AuNPs	Tap water	[33]
Aptamer-AuNPs	Cd (II)	Cd-Aptamer interaction promoted the aggregation of AuNPs	Drinking water	[42]
CuNPs-AgNPs-ternary matrix	Hg (II)	Variations in the intensity and shifts on the SPR bands	Drinking water	[37]
MT-CuNPs	Hg (II) and Pb (II)	Hg (II) and Pb (II) induced the aggregation of CuNPs	Tap and pond water	[39]
R-CuNPs	As (III)	The presence of As (III) promoted the release of R and the aggregation of CuNPs	Ground water	[40]

2.2. Nanocomposites for the Detection of Heavy Metals

The applications of nanomaterials are not only limited to colorimetric sensing; more sophisticated detection systems based on nanomaterials or with these incorporated have been investigated in recent years. In order to enhance the characteristics of detection, such as selectivity, specificity, and reproducibility, the fabrication of nano-sensor devices based on different nanocomposites represents a suitable option.

Unique metallic semiconductors and carbon-based electrodes with nanotechnology incorporated have been explored. Porous-activated carbon (PAC) decorated with palladium NPs (PdNPs) was used to fabricate a modified glassy carbon electrode (GCE). By using square wave anodic stripping voltammetry (SWASV), the activity of this modified electrode was applied in the detection of Cd^{2+}, Pb^{2+}, and Cu^{2+} ions with LODs of 13.33 nM, 6.60 nM, and 11.92 nM, respectively. The designed system exhibits peak currents related to the redox reaction in which the contaminant ions were reduced [43]. PAC in this system favored the speed of the electron transfer between the electrode and solution because of its porous structure, leading to better performance.

At the same time, using PdNPs improves the signal of detection thanks to their electrocatalytic activity and good conductivity. Moreover, the Pd@PAC/GCE was utilized

to detect heavy metal ions in natural sample species, indicating potential application in accurate environmental detection.

Modifying an electrode with a nanocomposite of zinc oxide nanorods (ZnO) and graphene (G) also generates the conditions for improved detection of Cd (II) and Pb (II). While graphene contributes properties of good conductivity, good electron transfer, and mechanical properties, the addition of ZnO allows the formation of a three-dimensional structure, which helps stabilize G and increases the surface area available for electrochemical detection [44]. An extra element was added to this sensing method based on the ZnO-G nanocomposite. The investigators demonstrate that the presence of Bi^{3+} can improve the detection performance by forming an alloy with Cd (II) and Pb (II).

The LOD reached using this designed platform was 0.6 μg/L for Cd (II) and 0.8 μg/L for Pb (II), and it proved effective in detecting these ions in actual wastewater samples.

A nanocomposite electrode, based on reduced graphene oxide (rGO) glycine and polyaniline, also exhibits excellent sensing properties for Cd (II) and Pb (II) detection in actual water samples. Different molecules combined on electrode surfaces enhance surface area, electron transfer rate, and affinity for the target contaminants [45]. The proposed sensor was applied for Cd (II) and Pb (II) detection with an LOD of 0.07 nM for Cd^{2+} and 0.09 nM for Pb (II) and showed good selectivity and reproducibility.

A modified electrode was designed to determine Pb^{2+} concentration by SWASV based on the same principles. By using a Fe_2O_3 NPs/ZnONRs/ITO electrode, while Fe_2O_3 NPs contribute to a higher electrocatalytic activity, ZnONRs ordered on the electrode improve the surface area and disposition of Fe_2O_3 NPs. The system showed high selectivity, good repeatability, and reproducibility, and the detection limit was 0.01 μM [46].

Electrodes designed to detect mercury, usually metallic NPs, have been used and performed better. Specifically, AgNPs and AuNPs, because of their catalytic activity, higher surface area, and the higher affinity of AuNPs for Hg (II).

Graphite pencil lead (GPL) covered with Au nano-dendrites was used to create a sensor surface for electrochemical detection of Pb (II), Cu (II), and Hg (II) with an LOD of 0.12, 0.19, and 0.18 ppb for each ion, respectively. The fabricated sensor proved to be an excellent tool for the simultaneous detection of these contaminants, as GPL is an easily obtainable and cheap material, and the fabrication technique of the sensor is simple, and achieved in less than a minute. The product exhibited acceptable sensitivity and reproducibility and could detect the three contaminants in actual water samples [47].

Although simple fabrication and multiple detection capacities are essential, the straightforward reading of the signal is also crucial to determine the potential applications of the developed sensors. Regarding this, Sebastian et al. [48] created a dual sensor for Hg (II) based on green synthesized AgNPs. In the investigation, the detection of the ion could be seen by the naked eye using the AgNPs alone or measured by cyclic voltammetry when AgNPs were used to elaborate a modified platinum electrode. When used alone in solution, AgNPs would aggregate in the presence of Hg (II) because of a complex formation suggested to be caused by the hydroxyl and thiol groups of glutathione present in the Agaricus spore extract and their interaction with mercury ions. This aggregation was detected as a color change in the solution, along with a decrease in the SPR absorption spectra of the solution, that occurred only in the presence of Hg (II). Because of the excellent selectivity exhibited by the green-synthesized AgNPs, they were applied to the surface of a platinum electrode. In this case, the detection of Hg (II) was carried out by cyclic voltammetry measures, where a clear peak was formed due to the redox reaction occurring in the presence of Hg (II). As in primarily AgNP-modified electrodes, the performance of the electrode was better when AgNPs were covering the surface, as they contributed to facilitating the diffusion and capture of the contaminant ion, improving the electrochemical response of the electrode. Both systems exhibited good selectivity, with a LOD of 2.1 nM for the electrochemical sensor developed.

Another innovation in the search for sensing application devices was modifying a paper electrode with nanomaterials to fabricate a Hg (II) sensor. The use of either carbon

nanotubes (CNTs) or graphene oxide together with AuNPs on the paper electrode surface results in a susceptible and selective sensor, as these combine the good conductance and stability of CNTs and GO with the improved sensing area and sensitivity conferred by AuNPs [49]. The highlight of this method for the fabrication of the device is the electrogeneration of AuNPs in situ over the modified electrode, ensuring its deposit on the surface and the sensor's good reproducibility. The described system detected Hg (II) in actual samples at a level comparable to screen-printed carbon electrodes and reached a detection limit of 30 nM.

A nanocomposite of PtNPs in conjunction with 3,3′,5,5′ tetramethylbenzidine (TMB) was used for colorimetric detection of Hg (II). Contrary to the other methods reviewed, in this case, PtNPs exhibit peroxidase activity, which would be observed by the color given by TMB, a chromogenic substrate [37].

Moreover, the addition of mercury ions would cause the aggregation of PtNPs and the reduction of their activity. Thus, the presence of mercury would be observed as an absence of color. Another innovation developed in this study relies on using a nanocomposite as a matrix that promotes the stability of NPs and their activity, increasing the precision of this method and their potential applications with different water sources [50]. The LOD reached 80 nM for Hg (II).

A Zn-based metallic organic framework (MOF) derived from 2-amino terephthalic acid was synthesized and characterized by Kumar et al. [51] for the detection and remediation of V^{5+} ions from wastewater. Due to the developed matrix's luminescence and water stability properties, the MOF exhibited an LOD of 220 nM while also proving proficient in removing the metal ion, with a maximum adsorption capacity of 460 mg/g. Arabbani et al. [52] developed an electrochemical sensor through sol-gel methods consisting of Ag/ZnO and zeolite imidazole frameworks (ZIF-8) nanocomposite. The surface area and porosity of the sensor allowed the detection of Hg (II) with high selectivity, featuring a linear range from 5–140 nM and a LOD of 40 nM.

An electrochemical sensor for the detection of Cu (II) was fabricated by Gao et al. [53], consisting of a stainless-steel mesh (SSM) and tungsten oxide (WO_3) composite. The sensor was developed to improve the detection mechanisms through preconcentration. Three SSM/WO_3 sensors with different morphologies were developed to determine the influence of the surface area in the detection and sensitivity of the nanocomposite, showing LODs in the range of 10–200 nM.

A green method for the synthesis of carbon dots and graphitic carbon nitride (GCN) composites was proposed by Radhakrishnan et al. [54] as a fluorescent sensor for the detection of metal ions. The sensitivity of the nanocomposite was pH-dependent in determining an optimal surface charge for detection. Thus, a LOD of 0.55, 0.18, and 0.3 nM for Cr (VI), Cu (II), and Pb (II), respectively, were obtained.

Sensors based on cation exchange reactions (CER) can also act as versatile tools for the detection of heavy metals in wastewater, as demonstrated by Bano et al. [55]. A ZnS-starch nanocomposite was synthesized and evaluated for the detection of Pb (II), Cu (II), and Hg (II), which was dependent on the signals, band gap, and coloration of the ZnS-metal interactions. The proposed method reported a LOD of 1, 10, and 1 µM for Pb (II), Cu (II), and Hg (II), respectively.

Cr (VI) treatment has also been explored using cellulose nanocrystals (CNCs). A chitosan/CNCs/carbon dots nanocomposite was formed by Zeng et al. [56], who assembled a porous structure to detect and remove Cr (VI). Carbon dots provided adsorption sites for the matrix, exhibiting an adsorption capacity of 218.8 mg/g. Further, the nanocomposite acted as a fluorescent probe for quantitatively detecting Cr (VI) with an LOD of 40 ng/L.

Table 2 summarizes the different nanocomposites discussed in this review for the detection of heavy metal pollutants.

Table 2. Summary of heavy metal detection by using different nanocomposites.

Nanocomposite	Heavy Metal	LOD (nM)	Polluted Matrix	Reference
Pd@PAC/GCE	Cd (II), Pb (II), Cu (II)	13.33 (Cd^{2+}), 6.60 (Pb^{2+}), 11.92 (Cu^{2+})	Tap water	[43]
ZnO-G	Cd (II), Pb (II)	0.05 (Cd^{2+}), 0.03 (Pb^{2+})	Wastewater	[44]
rGO-glycine-polyaniline	Cd (II) and Pb (II)	0.07 (Cd^{2+}), 0.09 (Pb^{2+})	Tap water	[45]
Fe_2O_3 NPs/ZnONRs/ITO	Pb (II)	10	Sea water	[46]
GPL-Au nano-dendrites	Pb (II), Cu (II), Hg (II)	57.8 (Pb^{2+}), 18.8 (Cu^{2+}), 60.1 (Hg^{2+})	Lake water	[47]
AgNPs-Agaricus Bispore-Platinum electrode	Hg (II)	210	Lake water	[48]
CNT-AuNPs-GO	Hg (II)	30	River water	[49]
PtNPs-TMB	Hg (II)	80	Lab water	[37]
Zn-based MOF	V (V)	220	Lab water	[51]
Ag-ZnO-ZIF-8	Hg (II)	40	Tap water, river water, orange juice	[52]
SSM-WO_3	Cu (II)	10	Lab water	[53]
Carbon dots-GCN	Cr (VI), Cu (II), Pb (II)	0.55 (Cr^{6+}), 0.18 (Cu^{2+}), 0.3 (Pb^{2+})	Tap water, pond water, river water	[54]
ZnS-starch	Pb (II), Cu (II), Hg (II)	1 ($Pb^{2+}$and Hg^{2+}), 10 (Cu^{2+})	Tap water, pond water	[55]
Chitosan/CNCs/carbon dots	Cr (VI)	20	Lab water	[56]

3. Nanomaterials for the Detection of Agrochemicals: Pesticides, Herbicides, and Insecticides

In addition to detecting heavy metals and ions, nanomaterials have been used to make sensors for different agrochemicals.

Agrochemicals are widely used to control insects, pests, and weeds, which results in notable increases in agricultural production. If the use of pesticides did not exist, there would be a considerable loss of 78% in fruit production, 55% in vegetable production, and 33% in cereal seed production [57]. Pesticides are also crucial in reducing diseases and increasing substantial crop yields. As pesticides are used to combat pests and control weeds using chemical substances, they are prone to becoming toxic to other organisms, affecting fish, birds, air, water, beneficial insects, non-target plants, soil, and essential crops.

Also, pesticides can be carried away from the target plants, resulting in environmental contamination and affecting human health [58]. The fact that products such as pesticides and insecticides are applied in such high quantities promotes their persistence and accumulation in wastewater and the agricultural products themselves. In addition, factors related to climate change also impact the application of pesticides and result in increased pesticide use and pesticide contamination [59,60].

Although international entities have established limits on acceptable concentrations of these agrochemicals, their detection is difficult and expensive, so as science advances, new ways are always sought to detect the presence of these substances more straightforwardly and quickly [61].

Currently, traditional methods are used for the detection of pesticides, which involve liquid chromatography (LC), detection cards (SC), and gas chromatography (GC). However, such methods involve expensive equipment, are time-consuming, and require much training. In that regard, advanced methods, such as sensors consisting of a broad spectrum of functionalized and modified structures, have been developed, featuring higher selectivity and sensibility than traditional methods [62].

One of the most prominent topics under study nowadays is electrochemical biosensors, consisting of enzymes, polymers, or aptamers, which have been widely studied to detect agrochemicals [63–65]. Further, these biosensors can also be modified with NPs or nanomaterials where a synergic effect might occur, enhancing their detection times and sensibility towards the desired analyte [66,67]. Electrochemical biosensors have also been of great interest due to their low cost, response, on-site analysis, and simple operation.

In contrast to bulk electrodes, the NPs located on the surface of electrodes enable rapid electron transfer kinetics and thus significantly increase the electroactive surface area, driving redox reactions to occur. The increase in the surface area enables lower LODs and higher analysis sensitivity. Mainly, NPs can increase the enzymatic load in the working area of the electrode since the surface-volume ratio increases the number of interaction sites, promoting more direct contact with the molecules presented by the enzymes [68,69].

This section highlights the detection of widely used agrochemicals that have been reported to present detrimental effects to the environment and human health, such as organophosphorous pesticides, carbamates, dithiocarbamates, glyphosate, and azine pymetrozine, using nanomaterials and nanostructured electrodes.

3.1. Nanomaterials for the Detection of Organophosphorous Pesticides

Chemically-modified nanostructured electrodes generate optimal use of the bioactive sites of, for example, enzymes, which are complex proteins that produce a specific chemical modification and thus facilitate the pathways for the adequate transfer of electrons. Among them, acetylcholinesterase (AChE)-based biosensors are the subject of a wide range of research to detect organophosphate (OP) pesticides [70,71]. This group of pesticides is known for its effects on living organisms by inhibiting AChE activity. OPs stand out among the most widely used classes of pesticides due to their toxic effects on vertebrates, which is why a wide variety of referenced research has been found.

The toxicity of OPs is due to the inhibition of the activity of acetylcholinesterase (AChE). This vital enzyme controls the transmission of nerve impulses to muscle and neuromuscular cells in living organisms [72]. Due to this, rapid, highly sensitive, and reliable measurement and detection of these pesticides become imminent and relevant. The detection of OPs is performed by AChE and involves its inhibition of the hydrolysis of acetylthiocholine (ATCh) using a specific potential [73]. Instruments for measuring biological or chemical parameters, called biosensors, based on the inhibition of AChE, are commonly used for identifying and quantifying pesticides. A disadvantage of this method is that it is not selective for different pesticides. However, it can provide information on the toxicological index it detects, determined as the total anticholinesterase load. Based on AChE, these biosensors are an excellent detection tool because they provide a rapid response, indicating the presence of contaminants in a sample. Further, the characteristics and properties of the pollutant are also assessed, which is vital for in situ measurements.

Determining a pesticide concentration can be achieved with optimal precision by monitoring the oxidation current of thiocholine (TCh) before and after inhibition. Despite the above, AChE-based biosensors can suffer from enzyme leaks and decreased sensitivity. Immobilization methods such as cross-linking, covalent bonds, or physical adsorption have been used for this purpose [74–76]. On the other hand, naturally occurring biopolymers are preferable for enzyme immobilization. For example, forming a system between agarose and guar gum allows the modulation of porosity, essential for adequate confinement of enzymes with minimal leaching. The advantage of the agarose and guar gum (A-G) compound is that it can form a fragile, transparent membrane with remarkable mechanical stability [77].

The analytical performance of the AChE biosensors has been reported to be improved through functionalization with noble metal NPs or rGO. Further, carbon nanotubes (CNT) have shown excellent electrocatalytic activity for thiocholine. Hence, this nanomaterial has been employed to develop and improve OPs detectors.

Using glass carbon electrodes (GCE) modified with amino-functionalized CNT, Yu et al. [78] created a highly sensitive biosensor for OPs in which AChE was immobi-

lized on the surface by its interaction with the amino group of CNT. The system was applied to detect paraoxon in plant samples that presented minor currents related to the concentration of the insecticide. The biosensor presented a desirable performance compared with the detection results obtained through GC analysis. The LOD was found to be 0.08 nM.

Moreover, modifying the GCE with CNT-NH_2 improved the system's sensitivity, as the NH_2 ensured good orientation of the AChE, improving the electron transference and, therefore, the detection and affinity of the sensor. AChE biosensors with AuNPs are fabricated using a non-electrolytic coating on vertical nitrogen-doped single-walled carbon nanotubes (VNSWCNT) for the detection of OPs [79]. The AChE was immobilized on AuNPs via Au–S bonding, and VNSWCNTs were produced by spontaneous chemical adsorption of NSWCNTs on a gold electrode, also via Au–S bonding.

Au/VNSWCNTs/AuNPs/AChE biosensors were used to monitor cabbage water, tap water, purified water, river water, and lake water using recovery tests. The methodology uses standard contents of 10^{-2} or 10^{-4} ppb of malathion. The analyses evidenced the recovery of the AChE biosensor, ranging between 95% and 105%.

Further, the results present a relative standard deviation (RSD) of 3.7%, indicating that the Au/VNSWCNTs/AuNPs/AChE biosensor presents optimal results due to a satisfactory application to detect OPs in actual samples and excellent application projections.

Manganese oxide (MnO_2) compounds can also be applied to the analysis to respond to the detection of pesticides [80]. The AChE enzyme catalyzes the acetylcholine chloride (ACh) molecule in this detection platform to produce the choline molecule. The product, in turn, is catalytically oxidized by the choline oxidase (CHO) molecule, synthesizing the betaine and hydrogen peroxide molecules. Research indicates that MnO_2 quenches the fluorescence of gold nanoclusters (AuNCs) due to the Förster resonance energy transfer effect. Thanks to the presence of AChE and choline oxidase, the substrate acetylcholine is catalyzed to generate H_2O_2 molecules and thus significantly induce the decomposition of MnO_2, complementing color change and fluorescence recovery. As an acetylcholinesterase inhibitor, the pesticide prevents the production of H_2O_2 and further blocks the breakdown of MnO_2, consequently producing a change in fluorescence. These prominent color and fluorescence responses identify and quantify pesticides [81].

An innovative device was designed as a bimodal fluorometric/colorimetric sensor with high precision for the detection of OPs. This was accomplished by developing a manganese dioxide nanocomposite anchored to a gold nanocluster (AuNCs-MnO_2), presenting excellent stability, using bovine serum albumin (BSA) as a co-mold. Considering that the fluorescence quenching effect induced by the MnO_2 compound can be reversed by the introduction of the AChE and CHO molecules, the AuNCs-MnO_2 composite was used to detect the reaction process of the enzymes [82].

One area of nanotechnology that is currently widely developed is research with single-walled carbon nanotubes (SWCNT), which is attracting attention to improve the performance of AChE biosensors due to their outstanding mechanical and electrochemical properties. The nitrogen atom is the optimal dopant for SWCNTs due to the sub-property of the atomic radius of nitrogen since the nitrogen atom has a similar radius to the carbon atom; thanks to this, it is easy to access the SWCNTs to form the C–N bond [83–85]. The nitrogen atom can also activate many adjacent carbon atoms, promoting electron transfer. The robust van der Waals force and π–π interaction can cause disorder and aggregation problems in SWCNTs. To avoid these problems, vertical SWCNTs (VSWCNTs) have been proposed, produced by spontaneous chemical adsorption of short SWCNTs functionalized with the thiol group on a gold electrode through the bonds between the Au-S atoms [86]. The maximum current property increases after the gold electrode is modified with VSWCNT. This is attributed to the fact that the VSWCNTs efficiently improve the activation of electron transport in the electrodes. The modified sensor increases its current significantly after the AuNPs are manufactured by the outstanding non-electrolytic coating on VNSWCNTs, attributing the notable increase in electrical conductivity to the AuNPs.

Due to the results mentioned above, Au/VNSWCNTs/AuNPs were considered the optimal feature-modified electrode with good results for subsequent experiments. The observed impedance curve of the Au/VNSWCNTs present in the investigation is significantly reduced thanks to the nitrogen atoms, which are proposed to activate adjacent carbon atoms to increase and promote the electron transfer of the SWCNTs.

The development of the AuNPs system by non-electrolytic coating on VNSWCNT made the impedance the lowest in these curves due to the synergy between AuNPs and VNSWCNT, which increased the in-plane sp_2 domains and significantly improved the electrical conductivity property of the VNSWCNT/AuNPs, corroborating previously reported results. These curves revealed that these data were consistent with cyclic voltammetry (CV) characterization. The current signals gradually decreased with increasing concentrations of Ops. This was attributed to the pesticides reacting with the active target groups of the AchE, which reduced the enzymatic activity. Furthermore, a direct linear relationship between the current and the concentration of Ops was determined. The biosensor that was developed showed excellent linear relationships at concentrations of 10^{-5} ppb, and the LOD was 3.05×10^{-6} ppb for methyl parathion, 1.97×10^{-6} ppb for malathion, and 2.07×10^{-6} ppb for chlorpyrifos [87].

After 28 days of storage, this AchE biosensor maintains the property at 95% of its initial current. The outstanding advantage of this biosensor is its excellent sensitivity and exceptional stability. This demonstrates that nitrogen doping promoted the electron transfer of the VSWCNTs and that the synergy between the AuNPs and the VNSWCNTs would improve the electrical conductivity and surface properties of the biosensor. Another notable feature of this biosensor is that it is enhanced by showing results of satisfactory recoveries to detect malathion in real samples, indicating excellent application prospects in the analysis and detection of Ops. These biosensors, VNSWCNT/AuNPs, present great research potential since their applications can be further expanded to immobilize other or different enzymes and various organic molecules, such as antibodies [88].

Another notable study that has been reported in prominent scientific publications is the development of magnetite NPs (MagNPs) with the modification of electrodes to analyze and detect OPs. A biosensor is proposed based on the interaction between AChE/CS/MagNPs and ATCh/malathion on the surface of a screen-printed electrode (SPE). Usually, after the determination, detection, and analysis of OPs, the developed and used electrodes are discarded. However, in recent methodologies presented in research, the MagNPs system is recovered by washing with water after removing the external magnet, and the SPE system is ready to be reused, or the idea can be extrapolated into other experiments.

A carbon-based screen-printed working electrode modified with 30 µL of AChE/chitosan/MagNPs was synthesized for the detection of OPs [89]. As an analysis, cyclic voltammograms were performed using a modified screen-printed carbon electrode and the AChE/chitosan/MagNPs system. It is essential to mention that the electrode does not show faradaic electrochemical processes, resulting in a PBS solution of 0.1 M at pH 7.4. Despite this, when incubated in PBS containing a concentration of 20 mM ATCh, electrochemical activity was observed as a result. The signal 0.41 V vs. Ag/AgCl corresponds to the oxidation of thiocholine, a product of the hydrolysis of ATCh catalyzed by AChE. After incubation of AChE/chitosan/MagNPs with 1.3 µM malathion, the maximum current that occurred decreased, indicating the notable inhibitory effect of the pesticide on AChE activity. Analytical curve results were obtained to determine malathion in a linear concentration range of 0.5 to 20 nM. LOD and LOQ were 0.3 and 0.8 nM, respectively. This research used the screen-printed carbon electrode modified with AChE/chitosan/MagNPs to detect malathion in tomato sauce and tap water samples, resulting in a 96.1 to 108.3% recovery. The proposed biosensor could be satisfactorily used for OP analysis and potential investigations.

Nanotechnological composites using metallic NPs and a metallic organic framework structure (MOF) present notable surface advantages of porosity and a high surface area; these properties have become promising material potential. One of the investigations, as mentioned above, consists of a MOF nanocomposite (UiO66-NH_2) based on amino-

functionalized Zr (IV) linked to PtNPs with properties of an increase in surface areas and highly diverse PtNPs for the selective detection analysis of OPs [90].

This nanostructured system, formed by Pt@UiO66-NH_2, provides more active chemical sites, which shorten the diffusion lengths of electrons and ions and improve the performance of the velocity property presented by the modified glass-carbon electrode. (GCE). Another advantage of Pt@UiO66-NH_2 nanocomposites is that they create stabilizing chemical microenvironments for AChE to detect OPs effectively and efficiently. Another research project that was carried out reports the use of CV and electrochemical impedance spectroscopy (EIS) to investigate the characteristic properties of the electron transfer of various electrodes. The results show that the highest reduction signals observed in the system developed using Pt@UiO66-NH_2 contrasted with other electrodes modified using nanoparticles [91].

As a result, it was observed that there was no maximum visible current for the bare GCE, UiO66-NH_2/GCE, or Pt@UiO66-NH_2/GCE system. On the contrary, an oxidation signal in the AChE/Pt@UiO66-NH_2/GCE biosensor stands out. This signal is produced by the active thiocholine that is produced by the hydrolysis of AChE. If malathion is absent in the solution, the substrate is catalyzed by AChE and becomes the thiocholine product. On the other hand, when malathion is present, the phosphorus atom of malathion first phosphorylates the serine residue of AChE found in the active site of AChE. After this, stable complexes that inhibit AChE activity are formed. Therefore, the OPs analysis and detection method consists of the principles of inhibition of AChE and oxidation of the thiocholine molecule.

The response produced by the differential pulse voltammetry (DPV) electrochemical technique of AChE/Pt@UiO66-NH_2/GCE shows, as a result, an oxidation signal at the working potential of 0.65 V. If the concentration of malathion is high, the maximum current result decreases. The LOD of malathion was 4.9, enhancing the improvement of electron transfer. In addition, these Pt@UiO66-NH_2 nanocomposites increase the surface area to load AChE through specific host-guest chemical interactions. The amine chemical groups used to functionalize UiO66 enhance the maintenance of the MOF's chemical stability property while anchoring the PtNPs, concluding that a favorable biosensor stability is produced.

Graphene is a sheet material synthesized from graphite. It has been classified as an attractive material for analyzing and detecting OPs. Graphene presents extraordinary electrical conductivity, sizeable mechanical strength, and a high specific surface area. Nevertheless, recent studies have shown the aggregation and restacking between graphene sheets caused by the van der Waals forces, hydrophobic interactions, and strong л–л stacking [92,93]. Aggregation and agglomeration can significantly reduce the high natural specific surface area that graphene presents, negatively influencing what happens for graphene's practical applications and research. To address this problem and provide a solution or improvement to the aforementioned, research proposes reassembling two-dimensional graphene sheets (2D-G) into three-dimensional graphene structures (3D-G) [94].

An innovative biosensor was developed with AuNPs/graphene using an electroless coating to eliminate and detect OPs. The 3D-G used nickel foam (NF) as a template and was combined with AuNPs to synthesize a three-dimensional AuNP/3D-G film, which features significant and notable advantages [95]. This simple and environmentally friendly film nanocomposite stands out because it has a large surface area for the adsorption of AChE to occur and thus improves and enhances the transfer of electrons and, simultaneously, the electro-oxidation signal of the thiocholine molecule. It is of great interest that integrating the AuNP/rGO system enhances a research area with new opportunities for rapid analysis and detection of OPs. Nafion is incorporated into the surface of AuNPs/rGO/GCE, forming the Nafion/AuNPs/rGO/GCE electrode system. The Nafion polymer molecule is a micellar polymer with excellent film adhesion capabilities, electrical conductivity, and biocompatibility properties, with various applications to encapsulate and stabilize enzymes. Moreover, AChE is added to the surface of the Nafion/AuNPs/rGO/GCE electrode system.

An EIS of GCE, rGO/GCE, and AuNPs/rGO/GCE were performed. As a result, the impedance of the naked GCE was at its maximum. On the other hand, the impedance of the AuNPs/rGO/GCE system was lower than that obtained from the rGO/GCE system and that of simple GCE. These results indicate that AuNPs improve conductivity properties and charge transfer performance. The electrochemical technique of differential pulse voltammetry (DPV) is also used to choose the optimal condition of the non-electrolytic AuNPs coating for the biosensors. As a result, the AChE/Nafion/AuNPs/rGO/GCE system exhibited much higher sensitivity than the AChE/Nafion/rGO/GCE system because the AuNPs facilitated electron transport and improved the conductivity property. The optimal conditions of synthesis, malathion, and methyl parathion are considered in a study as model-molecule pesticides and thus test the performance of the biosensor manufactured by DPV.

The AChE/Nafion/AuNPs/rGO/GCE systems were exposed to different chemical concentrations of malathion and methyl parathion in PBS solutions. The response given by the DPV exhibited an oxidation signal of 0.57 V that occurs due to the oxidation of the thiocholine molecule. Furthermore, the signal successively decreased with increasing chemical concentrations of malathion and methyl parathion, respectively.

The LODs were 2.78×10^{-11} g/L for malathion and 2.17×10^{-11} g/L for methyl parathion. As a result, the system presents good repeatability (4.07% relative standard deviation (RSD) and good reproducibility (RSD 5.3%). Storage studies were carried out over 35 days, resulting in the OPs biosensor retaining 83% of its initial response. In conclusion, there are various practical applications that the AChE/Nafion/AuNPs/rGO/GCE biosensor can present and were analyzed and studied through recovery tests carried out by adding methyl parathion to mineral water, tap water, and cabbage samples. The observed recovery values ranged between 93%–107%.

3.2. Nanomaterials for the Detection of Atrazine

One of the herbicides widely used and studied nowadays is atrazine. This agrochemical molecule draws attention due to its potential endocrine activity and carcinogenic effects. This agrochemical has low biodegradability in the environment, persisting for decades in soils. Therefore, this agrochemical passes into groundwater sources through rainwater. The conventional techniques currently used for analyzing and detecting atrazine involve techniques such as solid phase extraction followed by thin layer chromatography (TLC), HPLC, or combinatorial methods such as liquid chromatography-mass spectroscopy (LC-MS) or gas chromatography-mass spectroscopy (GC-MS) [96,97].

Advanced technologies have been developed for the detection of atrazine. Among them are plastic antibodies that are based on nanometric polymeric materials and can recognize a target organic molecule. This method, called molecular imprinting, aims to create or develop specific binding sites so that chemical recognition occurs and presents the form of the specific pesticide that is desired to be detected.

For example, affinity sensors prepared by attaching atrazine-imprinted poly(hydroxyethyl methacrylate-aspartic acid (HEMA-MA-aspartic acid) NPs onto the gold surface of surface plasmon resonance (SPR) sensor chips have been developed [98]. Further, an aqueous suspension of the NPs was dropped on the gold surface of the SPR chip. The main advantages of an atrazine-imprinted SPR sensor are its simplicity, high recognition ability, stability, and low cost.

The interaction of the NPs causes an increase in the hydrophilicity property due to the hydrophilic character of the polymeric structure. Image results from the scanning electron microscopy (SEM) characterization technique indicate that the NPs have a spherical shape and are uniformly distributed on the surface of the SPR chip, resulting in the formation of a self-assembled monolayer [99,100].

The simazine molecule was selected as a control to study and evaluate the present sensor's selectivity due to its molecular similarity with atrazine.

On the other hand, amitrole was chosen because the molecule is smaller than the atrazine molecule, which enhanced its inclusion in the printed nanocavities of the system. The results indicate that simazine and amitrole solutions cannot produce significant sensory responses despite their similarity and ease of access to the recognition cavities. The results obtained in these studies indicate that the atrazine molecule's recognition mechanism has chemical and physical interactions that must be provided together [101].

The printed SPR sensors recognized the atrazine molecule, presenting excellent selectivity due to chemical and shape recognition memory. One of the outstanding advantages of these SPR sensors printed with atrazine is that they are 8.17 and 25.5 times more selective for the agrochemical molecule of atrazine than for the molecules of simazine and amitrole. Furthermore, the sensor's response has the property and characteristic of reproducibility since it exhibited stable behavior during three use cycles. The SPR sensor prepared with the printing of atrazine molecules has excellent research and detection potential for environmental monitoring; this study can be extrapolated to other agrochemicals. The characterization results indicate that the molecular nanocavities formed in the molecularly printed polymer layer preferentially recognized the atrazine molecule, which corroborates that the cavities coincide more aptly with the size of the atrazine molecule than with simazine and amitrole. Finally, the results indicated the LOD and LOQ for the atrazine molecule and were determined as 0.71 ng/mL and 2.37 ng/mL, respectively.

3.3. Nanomaterials for the Detection of Carbamates and Dithiocarbamates

Another group of agrochemicals is of great environmental concern: pesticides with carbamate molecules as their active ingredient. Carbamates are organic molecular compounds derived from carbamic acid. Pesticide agrochemicals such as carbamates are currently used in agriculture to increase crop yields, as they have a high lethality for invertebrate animals such as insects. Unfortunately, carbamate residues destroy ecosystems and cause food contamination. Bioaccumulation effects in the human body are even more critical since pesticides composed of carbamates actively suppress or eliminate the activity of AChE, which plays crucial functions in the central nervous system and the body's peripheral system [102,103].

One of the essential advantages is that the ocular sensitivity is good enough to distinguish the apparent color variations for the quantitative detection of carbaryl, even if a concentration of 12.5 μg/mL is present. Rapid qualitative monitoring of carbaryl can be carried out with the proposed sensor with the naked eye, and a precise quantitative test is also carried out using spectrophotometry characterization techniques. The results indicate good selectivity and anti-interference behavior for the analysis and detection of carbaryl, even if presented in parallel with other commercial pesticides. A negative effect on carbaryl detection is due to common electrolytes and biological species. Therefore, the AuNCs-MnO_2 system presents great potential to monitor and detect the presence of carbaryl. Finally, carbaryl residues were analyzed in actual samples, obtaining recoveries between 90.3% and 111.7%.

On the other hand, dithiocarbamates (DTCs) are organosulfur compounds frequently used as agricultural pesticides and vulcanization additives and are known as wood preservatives in the rubber industry. DTCs are the most detected pesticides in monitoring programs. These agrochemicals can form metal complexes, and because of this, they act as enzyme inhibitors. DTCs primarily cause neurotoxicity, a degree of thyroid toxicity, and developmental toxicity in laboratory animals. It is necessary to quantitatively determine DTCs at low concentrations to reduce human exposure to the residues of these pesticides and environmental contamination of groundwater. Research reports different analytical procedures, which include characterization techniques such as spectrophotometry, chromatography, polarography, flow injection, biosensors, and advanced techniques such as LC-MS, HPLC-DAD, and GC-LC [104,105].

A simple and quick sensitive colorimetric detection of DTC pesticides (Ziram, Zineb, and Maneb) was described using sodium dodecyl sulfate (SDS)-capped AgNPs. The

color change is observed visibly by the naked eye and by a spectrophotometer [106]. The results from the absorption spectrum exhibited decreased SPR absorbance signals with bathochromic shifts due to the interaction of the sulfur atom of the DTCs with the AgNPs. The presence of disulfide functional groups makes the DTC compounds replace the surface ligands, which strongly interact with the surface areas of the noble metals and are chemically adsorbed on the outside of the AgNPs.

Furthermore, the negative sulfate ion fraction, SO_4^{2-}, of SDS can interact with the NH bond atoms of DTCs thanks to electrostatic forces and thus form a host-guest interaction. The ions Na^+, K^+, Mg^{2+}, Cl^-, CO_3^{2-}, and NO_3^- did not interfere. Tap water, vegetable juice such as tomato, and commercial drinks such as mango were used for analysis, and quantities of Ziram, Zineb, and Maneb, which were taken to study for analysis, were also added to the samples. As a result, the percentage of recovery was determined to be between 93%–108%. Finally, good sensitivity and selectivity values were obtained with an LOD between 4.01 and 149.27 ng/mL.

3.4. Nanomaterials for the Detection of Glyphosate

Glyphosate (N-(phosphonomethyl)glycine) and glyphosate-based agrochemicals are highlighted in the area as the most used herbicidal agrochemicals worldwide. They are non-selective, broad-spectrum herbicides used for the vital control of grasses when they are long and tall, in addition to the control of weeds with broad leaves. This agrochemical is used in highly excessive quantities in most crops, in periods just before harvest. The active ingredient, glyphosate, was considered controversial in Monsanto's Roundup herbicide due to its toxicity. Various studies have described various analytical methods, such as ion exchange chromatography, GC, HPLC, capillary electrophoresis, and different spectroscopic methods to detect glyphosate, which have certain advantages and few limitations [107,108]. However, enzyme inhibition-based biosensors stand out over the abovementioned techniques. These biosensors are based on the specific inhibition of the activity presented by the enzyme, which results in a reduced signal proportional to the target analyte. Researchers have attempted to develop a biosensor system using glyphosate since it eliminates most plants by inhibiting the urease enzyme. The enzyme urease is found ubiquitously in various varieties of plants and vegetables, has the property of being thermostable, and has activity in a wide pH range. Moreover, the quantification of enzymatic products occurs easily using potentiometry or direct photometry. The interaction and connection of NPs with enzymes for analysis and detection is a current and new topical approach to increasing the performance of biosensor systems based on urease, thanks to the synergistic effect of the two components. NPs offer many advantages due to their physicochemical and optical properties, in which the large surface-volume or surface-area ratio causes a high surface reaction activity and a strong adsorption capacity for biomolecules or biomolecular systems [109,110].

A nano-bioconjugate of urease with AuNPs was developed and immobilized in an agarose-guar gum matrix, which was employed for biosensing purposes. The immobilization efficiency of urease was 83%, while urease nanoconjugate showed an efficiency of 93% [111]. The response time for an ion-selective electrode covered with urease and urease nanoconjugate membranes was studied. 90% of the response was achieved in 3–4 min for the enzyme nanoconjugate, whereas the urease membrane took 7–8 min. The urease nanoconjugate membrane needed less time for stabilization.

The advantages and response characteristics of the electrode with the immobilized urease nanoconjugate can be attributed to the presence of AuNPs, which promote the efficient transfer of electrons in the reaction with the enzyme and enhance the sensitivity of detection. The proposed biosensor indicated, as a result, linear dynamic ranges from 0.5 ppm to 50 ppm of glyphosate concentrations with a LOD of 0.5 ppm.

The concentration of glyphosate that showed 50% inhibition (ID_{50}) of urease activity was around 45 ppm. Therefore, the manufactured biosensor can detect glyphosate below

the permissible concentration value (0.9 ppm) established by the World Health Organization (WHO) applied to drinking water [112].

Fourier transform infrared spectroscopy (FT-IR) analysis also confirmed the inhibition of the catalytic activity of urease in the presence of glyphosate. It is well known that phosphorodiamidates and imidazole are typical mechanism-based inhibitors of urease. Phosphorodiamidates have a P=O bond that tends to interact with the Ni ion in the active center of urease, further decreasing urea's binding to urease, leading to inhibition of urease activity [113,114]. Glyphosate (OH_2-PO-NH-COOH), being structurally similar to phosphorodiamidates (OH_2-PO-NH-R), may exhibit the inhibition of urease by a similar mechanism. A constructed biosensor was further tested for the detection of glyphosate in tap water samples. The values were obtained using a fabricated biosensor for tap water detection. Samples showed an average accuracy of 86% for the herbicide glyphosate.

Glyphosate detection based on urease nanoconjugates provides reasonable sensitivity on a broader concentration range with appreciable selectivity. It can detect glyphosate below the maximum residual limit (MRL) set by the Environmental Protection Agency (EPA, 0.7 ppm) and the World Health Organization (WHO, 0.9 ppm) in drinking water. The additional advantage of the present biosensor is its prolonged storage stability (180 days) [111].

3.5. Nanomaterials for the Detection of Triazine Pymetrozine

Another widely used agrochemical is triazine pymetrozine (PYM), an insecticide with high selective activity against homopteran insects, affecting their nervous regulation and feeding behavior. In addition, it presents low acute toxicity for humans, mammals, and birds. Despite these precedents, this agrochemical is classified as a potential human carcinogen, according to the information mentioned by the United States Environmental Protection Agency (EPA), and the national food safety standard has established a maximum level of 138 nM (0.03 mg/kg) present in foods [115].

The conventional detection methods for PYM include HPLC, LC-MS, GC, electronic spectroscopy, and differential pulse polarography (DPP) [116]. Although most of these methods offer suitable sensitivity to the detected materials, they are relatively complicated and time-consuming, with limited capacity for on-site detection in the field.

Researchers present an innovative, straightforward colorimetric sensor with high sensitivity and excellent selectivity for detecting PYM. The pesticide detection is based on the PYM-induced aggregation of AuNPs modified with the melamine material [117]. The LOD of the sensor for PYM is 80 nM for naked eyes and 10 nM for UV-visible spectroscopy, and the sensor reported here is applicable for rapid colorimetric detection of PYM in food samples and natural water environments.

The interaction of PYM, AuNPs, and melamine forms the complex system through hydrogen bonds. Subsequently, the melamine-AuNPs nanostructure agglomerated, causing a notable color change of the solution from red wine to blue, and this qualitative result is verified by the change in the SPR signal and its absorption intensity. If there is a low concentration of melamine, the AuNPs are well modified by melamine, and the assay's sensitivity could be more efficient. On the contrary, if the concentration of melamine is too high, the melamine-AuNPs agglomerate in the absence of potential analytes. As a conclusion to these results, the AuNPs were modified with 0.8 μM melamine. The selectivity property of this colorimetric sensor was evaluated qualitatively by observation with the naked eye and quantitatively using UV-visible spectroscopy, in comparison with other pesticides such as atrazine, glyphosate, iprodione, indoxacarb, MCPA-Na, fenobucarb, dipterex, pretilachlor, and isoprocarb. Because PYM has a specific chemical structure, the N-H functional group and the O atom of PYM interact with the amino functional groups of melamine through hydrogen bonds.

Due to these, the other pesticides, such as atrazine and iprodione, which were contained in the N atom and Cl atom, cannot form hydrogen bonds with the melamine material. Results show good linearity between A690 nm/A520 nm concentrations and

PYM, from 10 to 1000 nM, with an LOD close to 10 nM. This excellent linear response of the A690 nm/A520 nm ratio indicates that the melamine-AuNPs colorimetric sensor has the advantage of being useful in a threshold measurement and can also be used for a quantitative PYM assay. As a result, the melamine-AuNPs system indicates a lower LOD and a wider linear response range than any other colorimetric detection system reported to date in the present research. It presents excellent power in this area since it is an innovative method competitive with many other instrumental assays based on classical quantitative characterization methods such as electrochemical techniques, GC, or HPLC.

Examples of biosensors modified with enzyme-loaded nanoparticles discussed in this section can be found in Figure 3.

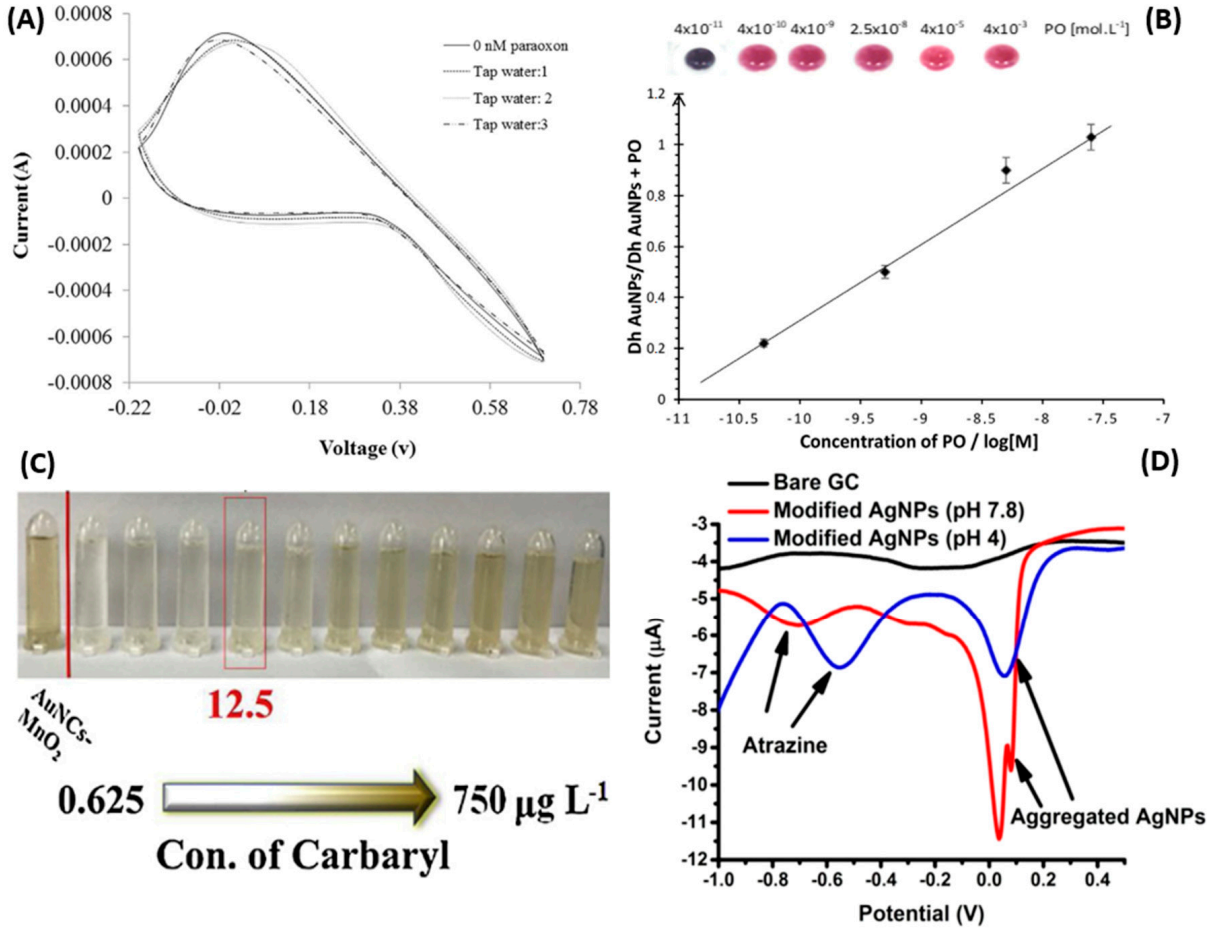

Figure 3. Detection of agrochemicals using biosensors modified with enzyme-loaded nanoparticles: Selective detection of paraoxon from actual tap water samples (**A**) [78]. Effect of increasing concentrations of paraoxon on the AChE-AuNPs biosensor (**B**) [76]. Colorimetric changes of an AChE-AuNCs-MnO_2 biosensor in the presence of increasing concentrations of carbaryl (**C**) [99]. Detection of atrazine through its oxidation when interacting with an AgNPs/GC modified electrode (**D**) [98].

Table 3 summarizes the different nanomaterials for agrochemical treatment that were discussed in this section.

Table 3. Summary of some examples of nanomaterials and nanocomposites that are used for agrochemical treatment.

System	Agrochemical	LOD (nM)	Polluted Matrix	Reference
AChE-CNT-GCE	Paraoxon	0.08	Vegetable samples	[78]
VNSWCNTs/AuNPs/AChE	Malathion	0.3	Cabbage samples	[79]
Au/VNSWCNTs	Methyl Parathion, Malathion, Chlorpyriphos	0.03 (methyl parathion), 0.01 (malathion), 0.03 (chlorpyrifos)	River water	[81]
AChE/CS/Fe_3O_4	Malathion	0.3	River water	[84]
Pt@UiO66-NH_2 nanocomposite	Malathion	4.9×10^{-6}	Garlic samples	[85]
Nafion/AuNPs/rGO/GCE	Malathion and Methyl Parathion	0.08 (malathion), 0.07 (methyl parathion)	Cabbage sample, tap water, river water	[95]
HEMA-MA-aspartic acid-AuNPs	Atrazine	3.3	Lab water	[98]
BSA-stabilized AuNCs-MnO_2	Carbaryl	0.63	Lake water, soil	[99]
SDS capped AgNPs	Ziram, Zineb, and Maneb	0.03–0.57	Lab water	[101]
Urease-AuNPs agarose-guar gum	Glyphosate	1.8	River water	[113]
Melamine-modified AuNPs	Triazine Pymetrozine	10–80	Tap water, lake water	[76]

4. Cyclodextrin-Based Materials and Cyclodextrin Polymers for the Remediation and Detection of Pollutants

4.1. Cyclodextrin Monomers and Cyclodextrin-Based Polymers

Cyclodextrins (CDs) are cyclic oligosaccharides synthesized by enzymatic starch reactions with the amylase of *Bacillus macerans*. Among them, β-CDs stand out due to their cavity dimensions (7.8 A), which can suitably accommodate organic compounds of suitable size to form inclusion compounds through host-guest interactions [118–120]. Some examples of guests that have established supramolecular interactions with CDs are heavy metals, dyes, pesticides, and organic pollutants [121–123].

Furthermore, CDs have high reactivity because their hydroxyl groups can undergo elimination or substitution. CDs have been used to form crosslinked polymers because of their well-defined structure, moderated toxicity when administered locally or orally, and versatility. This reticulated structure formed by co-polymerization exhibits multiple nanochannels, which allows the loading and solubilization of both hydrophilic and lipophilic molecules [124,125].

4.2. Potential Applications of CD Monomers and CD Polymers in Environmental Remediation

Due to the abovementioned properties, CDs and their polymers (also known as cyclodextrin nanosponges, NSs) present several advantages in environmental remediation, showing high percentages of pollutant removal from wastewater. It is noteworthy that, in the case of CD-based polymers, the inclusion of the pollutants not only occurs by host-guest interactions but also by diffusion through the multiple pores and interstices in the sponge-like network, which are formed in the polymerization reaction [126]. Moreover, assembled βCD monolayers (βCDMs) on surfaces represent an interesting research topic in areas like analytics detection because they offer a unique way to confine molecules in two dimensions by controlling binding events on the interface [127].

The arrangement of βCDMs can act as a template for molecular recognition where intermolecular matrix-host interactions are reversible, which means that βCDMs can include and release the invited molecules. The following sections discuss the sorption mechanisms, removal efficiencies, and detection of pollutants using CDs and CDs-based polymers. The potential applications of the CDs-modified materials and the CDs-based polymers in environmental remediation are summarized in Figure 4.

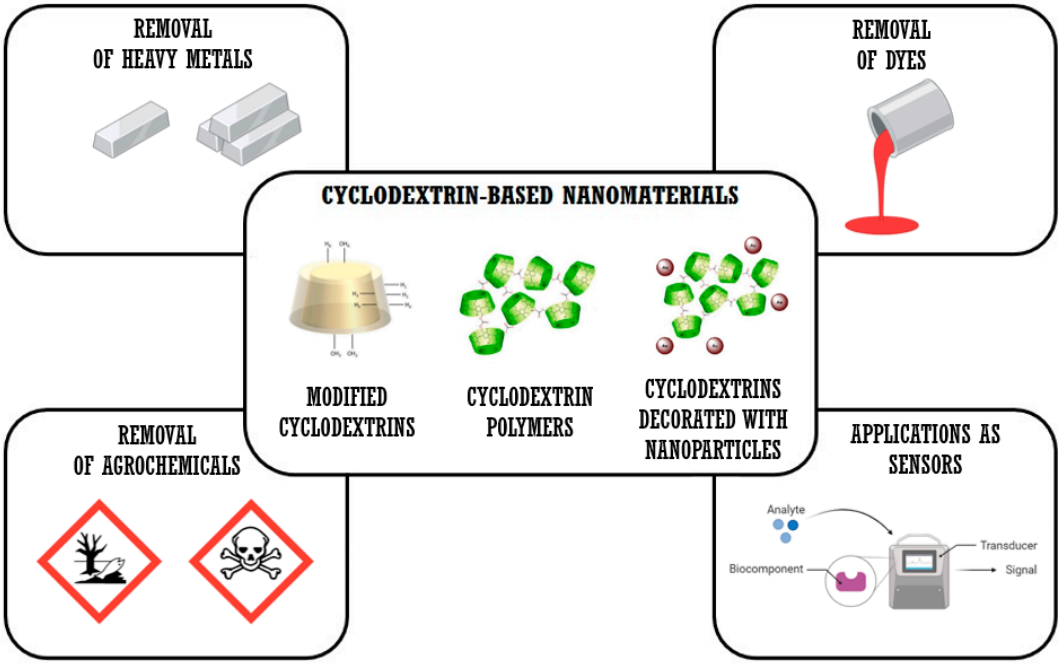

Figure 4. Schematic representation of CDs-based materials and their potential applications in environmental remediation and detection. Created with BioRender.com.

4.3. CDs Monomers and CD-Based Polymers in the Remediation of Heavy Metals

Heavy metals are naturally occurring elements with a higher molecular weight and density than water. Heavy metals have multiple applications, such as industrial, domestic, agricultural, medical, and technological. As such, their distribution in the environment is wide. This raises concerns because of their high toxicity and easy absorption by living organisms, leading to bioaccumulation and severe conditions such as mental disability, dementia, and vision problems. CDs and CD-based polymers have been reported for the removal of a broad range of heavy metals, such as Cr, As, Ni, Co, Hg, and Zn.

A nanocomposite of β-CD-chitosan-Fe_3O_4 was developed to remove arsenite ions from an aqueous solution [128]. The adsorption capacity, kinetics, and mechanisms of removal were determined, as well as the optimal conditions for arsenite removal.

The uptake of arsenite reached a value as high as 96%, ascribed to the hydroxyl and amine groups present in the polymer, with the Fe_3O_4 NPs playing a vital role in the enhanced adsorption of As^{3+} ions as well. Sorption of arsenite ions has also been performed using permethylated β-CD-impregnated resin [129]. Optimal pH and concentration conditions were also determined to reach a maximum removal efficiency of 98%. Adsorption capacity and reusability of the β-CD-based resin were also reported.

A β-CD functionalized three-dimensional structured graphene foam (CDGF) was synthesized with a one-step hydrothermal method for the removal of Cr (VI) from wastewater. The CDGF system showed good selectivity at pH = 3 in comparison with other heavy metals. FT-IR and XRPD characterization analyzed the sorption mechanism, thus determining that the hydroxyl groups present in CDGF promote the removal of Cr (VI) [130].

A new composite material consisting of β-CD functionalized on the surface of magnetic nanotubes was developed to remove Ni (II) ions [131]. This system removed the heavy metal effectively, with a maximum adsorption of 103 mg/g at room temperature. The sorption mechanisms were also discussed, where the host-guest interactions occurring between β-CD and Ni were estimated to be the main adsorption force, with Fe_3O_4 being a determinant in the capture of Ni as well.

An EDTA-functionalized β-CD-chitosan composite was synthesized via a two-step process for the removal of heavy metals such as Pb (II), Cu (II), and Ni (II). Isotherm studies depicted high removal efficiencies for all metallic ions. Furthermore, the novel adsorbent

showed excellent adsorption capacities even in the presence of other pollutants such as ciprofloxacin [128].

Pyromellitic cyclodextrin nanosponges (NSs) were prepared by reacting β-CD with pyromellitic dianhydride (PMDA) in dimethyl sulfoxide (DMSO) for the adsorption of heavy metal cations and comparing their removal efficiency with that of citric nanosponges. At lower concentrations of metals (<50 ppm), both the citrate and pyromellitic NSs showed about the same retention capacities for Cu (II), Zn (II), Pb (II), Cd (II), and Fe (III). In contrast, the adsorption capacity of the pyromellitic NSs was higher at metal concentrations of 500 ppm. However, in the presence of interferences, the citrate NSs showed higher selectivity, especially in the case of Cu^{2+} [132].

A novel β-CD covalently-crosslinked tannic acid NSs via condensation method was synthesized via a condensation reaction for the selective capture of Pb (II). The hydroxyl groups in the nanosponge could bind effectively with Pb^{2+}, providing selectivity over coexisting metals (selective coefficient of 1143). Also, an ultra-fast removal efficiency of 81% within 3 min was reached [133].

A summary of relevant studies on CD-based materials and their potential applications for the removal of heavy metals is presented in Table 4 as follows:

Table 4. Summary of relevant data on CD-based materials and results concerning the treatment of heavy metals in aqueous media.

System	Heavy Metal	Maximum RE (%) or Adsorption Capacity (mg/g)	Optimal Conditions: pH, Metal Concentration, Contact Time	Reference
β-CD-chitosan-Fe_3O_4	As (III)	96%	pH 9, 0.1 mg/L, 20 min.	[129]
Permethylated β-CD	As (V)	98%	pH 6, 0.1 mg/L, 30 min.	[130]
β-CD-graphene foam	Cr (VI)	99.8%	pH 3, 50 mg/L, 240 min.	[131]
β-CD-CNT-Fe_3O_4	Ni (II)	103	pH 6, 50 mg/L, 50 min.	[128]
β-CD-chitosan-EDTA	Pb (II), Cu (II), Ni (II)	330.9 (Pb^{2+}), 161 (Cu^{2+}), 118.9 (Ni^{2+})	pH > 5, 25 mg/L, 300 min.	[132]
PMDA-β-CDNSs	Cu (II), Zn (II), Pb (II), Cd (II), and Fe (III)	Up to 94%	pH not reported; 500 ppm, 24 h.	[133]
Tannic acid β-CDNSs	Pb (II)	81%	pH range 4–6, 200 mg/L, 3 min.	[134]
Citric acid β-CDNSs	U (VI)	150	pH 4; 60 mg/L, 60 min.	[134]
Calixarene-CDNSs	Pb (II)	Up to 85%	pH > 6, metal concentration not reported; 5–10 min.	[135]
Citric acid βCDNSs-ZrO_2	Pb (II)	274.5	pH 7, 200 mg/L, 120 min.	[136]

4.4. CDs Monomers and CD-Based Polymers in the Remediation of Dyes

Synthetic dyes are widely used in industries, mainly textiles, ink, and paper. Most dyes and their metabolites are toxic and carcinogenic to humans and living organisms. Furthermore, dyes are generally water-soluble compounds, thus making their removal from water sources difficult. CDs and their polymers have shown promising results in removing dyes from wastewater.

β-CD-EPI-magnetic NSs were synthesized and characterized for removing the azo dye Direct Red 83:1 from wastewater [137]. The results showed that 0.5 g of NSs and a pH of 5.0 were the optimal conditions for carrying out kinetic and isotherm models. Moreover, the polymer showed good reusability and was complemented with pulsed light and hydrogen peroxide to degrade the dye.

Eliminating dyes from the water was also accomplished by adsorption using NSs elaborated with β-CD with 1,2,3,4-butane tetracarboxylic acid as a cross-linker in the presence of PVA [138]. The NSs reached a maximum removal of 98%, and 96% for malachite green and safranin, respectively; each dye had an initial concentration of 25 mg/L. Notably, the reusability after five regeneration cycles evidenced 94.6% and 91.6% for malachite green

and safranin adsorption, respectively, confirming the feasibility of the abovementioned system as a potential method for dye removal.

All native CDs, α, β, and γ-CDs, were used as precursors to synthesize NSs, where epichlorohydrin (EPI) acted as a cross-linker [139]. The three cyclodextrin-based polymers were used as adsorbent materials to remove Direct Blue 78 from wastewater. The formation of inclusion complexes between the EPI-NSs was compared with that of native CDs. All polymers showed promising results in removing the dye from the solution, as the maximum efficiencies in Direct Blue 78 removal were as high as 99% for β-CD-EPI NSs and about 97% for α and γ-CD-EPI NSs. The sorption properties of the polymers were ascribed to the inner cavities of the CDs monomers and the porous surface produced in the polymerization reaction.

Insoluble NSs were covalently grafted with phosphorylated carbon nanotubes (CNT) and decorated with TiO_2 and AgNPs as a biosorbent for Congo red from wastewater samples [140]. The solution pH, adsorbent dosage, isotherm, and desorption studies were analyzed to determine the best conditions for Congo red removal, reaching maximum adsorption of 146.96 mg. Regeneration cycles and the adsorption mechanism of the developed polymer were also explored.

β-CD polymers generated on the surface of reduced graphene oxide (rGO) were prepared for organic dye adsorption [141]. The maximum adsorption capacity of the polymer-coated system was evaluated with malachite green (88.7%), as well as the recyclability of the adsorbent. Further, parameters for adsorption, namely pH, contact time, adsorbent amount, and temperature, were all investigated and optimized.

Results regarding the removal of dyes using recently developed CD-based technology are summarized in Table 5:

Table 5. Summary of studies regarding the treatment of dyes using CD-based materials.

System	Dye	Maximum RE% or Adsorption Capacity (mg/g)	Optimal Conditions: pH, Contact Time	Reference
EPI NSs-Fe_3O_4	Direct Red 83:1	>90%	pH 5, 30 min.	[138]
1,2,3,4-butane tetracarboxylic acid NSs	Malachite Green and Safranin	98.3% for Malachite Green, 96% for Safranin	pH 8, 180 min.	[139]
α-CD-EPI, β-CD-EPI, γ-CD-EPI	Direct Blue 78	99% (β-CD-EPI); 97% (α-CD-EPI, γ-CD-EPI)	pH 6, 120 min.	[140]
NSs-CNT-TiO_2-AgNPs	Congo Red	146.7	pH 8, 450 min.	[141]
β-CD-EPI-rGO	Malachite Green	902.2	pH 8, 90 min.	[142]
Halloysite-CD-NSs	Rhodamine B	70%	pH > 4.5, 100 min.	[142]
β-CD-DPC NSs	Basic Red 46 and Rhodamine B	101.3 (Basic Red); 52.3 (Rhodamine B)	pH 3–5, 120 min. for Basic Red; 180 min. for Rhodamine B	[124]
Citric Acid β-CD NSs	Methylene Blue and Congo Red	5.1 for Methylene Blue; 12 for Congo Red	pH not reported; 1500 min. for Methylene Blue; 40 min. for Congo Red;	[143]
β-CD-Activated Charcoal-Alginate-Fe_3O_4 nanocomposite	Methylene Blue	99.53%	pH 6, 90 min.	[144]

4.5. CDs Monomers and CD-Based Polymers in the Remediation of Pesticides and Agrochemicals

Organic compounds, such as pesticides and agrochemicals, are widely present in water sources due to anthropogenic activities. Pesticides and agrochemicals are extremely toxic to human health. These compounds are applied extensively worldwide to kill pests and are not only used in agricultural fields but also in homes, parks, schools, and buildings. This makes organic pollutants ubiquitous in the air we breathe, the water we drink, and the food we eat. Toxicological studies suggest pesticides and agrochemicals can cause health issues, such as ocular irritation and weight loss.

CDs-based polymers are a great tool to remove organic pollutants from wastewater, as reported in the following studies.

The sorption properties of β-CD-based NSs synthesized with diphenyl carbonate (DPC) as a linker were evaluated with the pesticides 4-chlorophenoxyacetic acid (4-CPA) and 2,3,4,6-tetrachlorophenol (TCP) and compared to materials such as granulated activated carbon (GAC) [145]. NSs could efficiently form inclusion complexes with both pesticides, outperforming GAC. NSs also proved to be an optimal substrate for stabilizing magnetite NPs, improving the properties of the polymer. Similar results were obtained using the same CD-based polymer and dinotefuran (DTF) as guests. [146].

β-CD-modified cellulose nano-fiber membranes have been fabricated to remove bisphenol pollutants (bisphenol A, bisphenol S, and bisphenol F) from water [147]. The systems were evaluated in actual water samples, such as lake and river water. The complete removal of the bisphenol pollutants confirmed the possibility of the β-CD cellulose membrane for potential applications.

Polycyclic aromatic hydrocarbons (PAHs) were removed from wastewater to develop a sorbent platform based on hypercrosslinked hydroxypropyl-β-CD networks, produced by electrospinning highly concentrated hydroxypropyl-β-CD solutions containing 1,2,3,4 butane tetracarboxylic acid as cross-linker [148]. This CD-based polymer demonstrated high sorption performance and was produced using green methods.

Utzeri et al. described the synthesis and characterization of CD-based NSs using two uncommon crosslinkers: hexane-1,6-diamine (am6) and dodecane-1,12-diamine (am12). The crosslinkers highly influenced the physicochemical properties of the synthesized NSs. The studies proved the am6-NSs to be a better sorbent for imidacloprid, also considering other parameters such as imidacloprid concentrations, the volume of solution, pH, and the amount of NSs [149].

B-CD and γ-CD-based polymers synthesized with epichlorohydrin (EPI) were associated with MnO_2 nanorods to provide a rigid material for the sorption of organic contaminants. The materials showed high removal efficiency and stability towards pesticides such as atrazine, benalaxyl, bromacil, butachlor, fenamiphos, fipronil, flufiprole, and pretilachlor.

The γ-CD polymers outperformed the β-CD polymers in terms of the sorption capacity of fipronil, benalaxyl, and fluliprole, due to the higher hydrophobicity and larger molecular weight. However, β-CD polymers demonstrated higher adsorption capacities than the other pesticides [150].

CD-based NSs were synthesized with 1,1′-carbonyldiimidazole (CDI) or pyromellitic dianhydride (PDA) to counteract the herbicide effects of Ailanthone, with γ-CD-NSs with CDI as crosslinker providing the highest loading capacity and encapsulation efficiency among the proposed NSs [151]. The use of the CD-based polymers demonstrated that the phytotoxic activity of Ailanthone can be increased or decreased.

Anionic CD polymers obtained from the crosslinking between citric acid, β-CD, and PVA were prepared for cationic pollutant removal from an aqueous solution [152]. The polymer exhibited a removal rate of 91% for paraquat, 97% for methylene blue, and 98% for crystal violet. The system also showed outstanding recyclability performance after five cycles of reuse. The removal of the agrochemical paraquat using a β-CD polymer with 1,2,3,4 butane tetracarboxylic acid as a cross-linker was achieved by Martwong et al. with similar results [153]. Both NSs were used for the coating of a cotton cord to develop a modified textile as a means of adsorbent.

Poly β-CD composites were synthesized and characterized by Utzeri et al. to assess their adsorbing properties by using cymoxanil and imidacloprid pesticides [154]. The composites reached removal efficiencies of nearly 80% for both substances, and their sorption/desorption cycles were also evaluated with good results.

A summary of various CD-based materials developed and investigated for potential applications in wastewater treatment and organic pollutants removal is presented in Table 6.

Table 6. Studies related to the application of CD-based materials in the treatment of organic pollutants.

System	Organic Pollutants	Maximum Removal Efficiency	Optimal Conditions: pH, Contact Time	Reference
DPC NSs-Fe_3O_4	4-chlorophenoxyacetic acid and 2,3,4,6 tetra chlorophenol	91% for 4-CPA, 78% for TCP	pH 9, 120 min.	[146]
DPC NSs-Fe_3O_4	Dinotefuran	90.3%	pH 7, 120 min.	[147]
β-CD-cellulose nanofiber	Bisphenol A, Bisphenol S, Bisphenol F	88.1%	pH 7, 15 min.	[148]
Hydroxypropyl β-CD-1,2,3,4 butane tetracarboxylic acid NSs	PAHs	92% (initial concentration of 400 μg/L of PAH) and 89% (initial concentration of 600 μg/L of PAH)	pH 7, 60 min.	[149]
Am6-NSs and Am12-NSs	Imidacloprid	95%	pH 3.8, contact time not reported	[150]
β-CD-EPI NSs and γ-CD-EPI NSs functionalized with MnO_2 nanorods	Atrazine, benalaxyl, bromacil, butachlor, fenamiphos, fipronil, flufiprole, and pretilachlor	Ranging between 43%–73%	pH 7, 120 min.	[151]
CDI NSs and PDA NSs	Ailanthone	55.1%	pH not reported; 24 h.	[152]
Anionic β-CD-citric acid NSs-cotton cord	Paraquat, Methylene Blue, and Crystal Violet	91% (Paraquat), 97% (Methylene Blue), 98% (Crystal Violet)	pH 6 for Paraquat; pH 4 for Methylene Blue and Crystal Violet, 360 min.	[153]
Anionic β-CD-1,2,3,4, butane tetracarboxylic acid NSs-cotton cord	Paraquat	95.1%	pH 8, 360 min.	[154]

4.6. CDs Monomers and CD-Based Polymers as Electrochemical Sensors

CDs and their polymers have been developed as selective sensing platforms as an analytical method for ultra-trace detection of pollutants.

A thiolated β-CD-decorated gold nanosatellite substrate was developed as a surface-enhanced Raman scattering sensor for the selective detection of bipyridinium pesticides, namely paraquat, diquat, and difenzoquat. The LOD of the pesticides was 0.05 ppm for each. Also, selective bipyridinium detection was performed by comparing the Raman spectra of each pesticide before and after washing the substrate [155].

A voltametric sensor consisting of L-citrulline and β-CD-modified glassy carbon electrodes was built to quantify and detect metribuzin. The proposed sensor displayed ultra-low detection limits of 10 nM and high specificity. The sensor also showed satisfying results using actual samples, implying that the novel system could be potentially used for environmental applications [156].

An electrochemical sensor consisting of Mxrene/carbon nanohorns/β-CD metal-organic framework (MOF) was developed as a sensing platform for pesticide carbendazim determination [157]. The β-CD-MOF combined the properties of both matrices, displaying the host-guest recognition of β-CD and the porous structure, high porosity, and pore volume of MOFs, enabling the adsorption of the pesticide. The synergic effect of β-CD and MOF provided a low detection limit (1.0 nM), high selectivity, and long-term stability.

A porous fluorescent polymer composed of β-CD, 4,4′-diisocyanate-3,3′-dimethyl biphenyl (DL), and tetrakis (4-hydroxyphenyl) ethene (TPE) was designed for the rapid and controlled detection of nitroarenes, namely trinitrophenol and nitrobenzene, in aquatic environments [158]. This work demonstrated that nitroarene compounds' "on-off" fluorescence detection might have field-based applications.

Polyvinyl chloride (PVC) membrane sensors have been constructed to determine procainamide. The sensors incorporated α, β, and γ-CD as ionophores, with the reaction mechanisms based on the formation of inclusion complexes [159]. The determination of procainamide showed high recovery, high stability of the formed complexes, and free from interferences. Similar studies with PVC-CDs membranes were carried out using the pesticide trazodone as a guest, showing good selectivity for trazodone in the presence of different ionic compounds [160].

Table 7 shows a summary of recent data concerning the use of CD-based materials as sensors for the detection of pollutants.

Table 7. Data on CDs-based materials and their applications as electrochemical sensors.

System	Organic Pollutants	LOD (nM)	Linear Range (nM)	Reference
Thiolated β-CD-gold nanosatellite	Paraquat, Diquat, Difenzoquat	18.5	18.9–37.8	[156]
L-Citrulline-CD-glassy carbon electrode	Metribuzin	10	0.03–1	[157]
β-CD-MOF-Mxrene-Carbon nanohorns	Carbendazim	1	3–10	[158]
Fluorescent β-CD-DL-TPE	Trinitrophenol and nitrobenzene	5	10–150	[159]
α-CD, β-CD, and γ-CD on PVC matrix	Procainamide	240, 213, 238 for α-CD, β-CD, and γ-CD, respectively	0.01–1.0	[160]
β-CD and γ-CD on PVC matrix	Trazodone	2.2 (β-CD) 0.15 (γ-CD)	7–100 (β-CD) 0.5–100 (γ-CD)	[161]
β-CD incorporated into graphene/ poly(dimethyl siloxane) composites	Propylparaben	10	10–100	[161]
Poly pyrrole nanotubes-β-CD-TiO_2	Methylparaben and Methylene Blue	10	10–100	[162]
rGO-β-CD-glassy carbon	Catechol	1.3	100–800	[163]

Examples of CDs monomers and CDs-based polymers for the remediation and detection of pollutants are summarized in Figure 5.

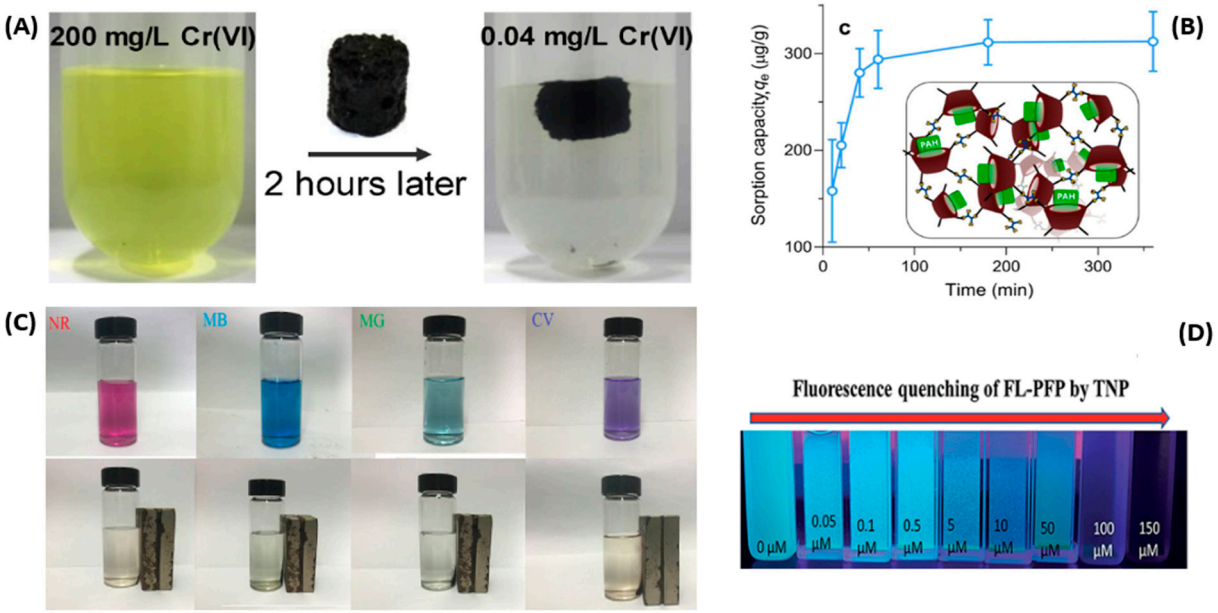

Figure 5. Remediation and detection of pollutants using CDs monomers and CDs-based polymers: Solid-liquid separation strategy for the removal of Cr (VI) using a β-CD functionalized graphene (**A**) [131]. Adsorption capacity of nanofibrous CDs membranes during the removal of PAHs (**B**) [149]. Images of pollutants (natural red, NR; methylene blue, MB; malachite green, MG; crystal violet, CV) before and after adsorption using a Fe_3O_4-NSs composite and subsequent magnetic recollection (**C**) [138]. Fluorescence quenching at increasing concentrations of trinitrophenol using a fluorescent β-CD terpolymer (**D**) [159].

5. Nanomaterials for the Remediation of Pharmaceutical Pollutants

Another matter of concern is the occurrence of pharmaceutical pollutants in the environment. Pharmaceutical effluents are classified as emerging pollutants due to the inability of wastewater plants to remove them effectively [164,165]. The impacts of such toxic materials at trace levels are also unclear, making the development of new technologies for their removal and treatment imperative [166,167]. Pharmaceutical pollutants are diverse, encompassing toxic materials such as antivirals, antibiotics, steroids, and painkillers. Their presence in the environment threatens humans, animals, and plants, which can result in endocrine disruption, cardiovascular disorder, and cytotoxicity, even at the levels of ng/L [168].

Although diverse methods for removing pharmaceutical pollutants have been described, such as oxidation or degradation, adsorption using nanostructured materials has been employed in recent years, reaching high removal efficiencies in mild experimental conditions with short contact times.

Martínez et al. [169] demonstrated the adsorption of ibuprofen using silver/magnetite core-shell nanoparticles (Fe_3O_4@AgNPs). A removal efficiency of 93% was achieved within 45 min, which was retained after three adsorption/desorption cycles. The adsorption studies were performed under neutral pH and room temperature in actual water samples, further confirming the nanomaterial's suitability for removing the emerging pollutant.

The removal of ibuprofen from wastewater was also studied by Chahm et al. An adsorbent consisting of a chitosan/γ-Fe_2O_3 nanocomposite was developed [170], obtaining a maximum adsorption capacity of 395 mg/g at room temperature and pH 7. The data also evidenced the recyclability of the proposed material, using ethanol for the adsorption/desorption cycles.

Priyan et al. assessed the viability of using starch nanoparticles to remove ibuprofen and sulfamethoxazole from wastewater [171]. The drug adsorption conditions were studied and optimized, reaching maximum removal efficiencies of 86% at an acidic pH using an adsorbent concentration of 0.01 mg/L. Further, the toxic effects of both drugs on seeds and zebrafish were analyzed, increasing the LD_{50} 7-fold after adsorption.

Chemically modified multi-walled carbon nanotubes (MW-CNTs) were synthesized by Yanyan et al. to remove acetaminophen from wastewater [172]. The surface of the MW-CNTs was treated with NaOH, ozone, chitosan, and HNO_3/H_2SO_4. The modified MW-CNTs outperformed the pristine structure, in which the ozone-MW-CNTs had superior adsorption efficiencies (250 mg/g). However, it was concluded that the effluent could not meet the allowed limit in wastewater set by legislation (<0.2 mg/L), suggesting the necessity of complementing the removal of acetaminophen with biological methods.

TiO_2 nanocomposites have also proven to be effective in removing acetaminophen. As Tao et al. reported, TiO_2-graphene material was synthesized through hydrothermal methods [173]. The BET surface areas of the TiO_2-graphene nanocomposite were more significant than those of the pure components, which provide more active sites for removing the drug pollutants. A removal efficiency of 97% after 180 min was achieved, which was pH-dependent.

A ternary maltodextrin/graphene oxide/copper oxide nanocomposite was proposed by Moradi et al. [174] for the removal of emerging pollutants diclofenac and amoxicillin. The highest removal efficiency was 95%, obtained at previously determined optimal conditions: pH 7, an adsorbent dose of 0.05 g, and an adsorption time of 7 min at 20 °C.

Two nanocomposites were developed by Tran et al. In their first work, the removal of diclofenac from wastewater using a cobalt-based ferrite ($CoFe_2O_4$) and graphene oxide system was achieved [175]. The adsorption experiments were evaluated at optimal conditions (pH 4, adsorbent dose of 7 g/L, 120 min). It was also concluded that the decoration of CoFe2O4 with graphene oxide provided functional groups essential for interacting with diclofenac. The second work proposed the formation of a carbon-coated magnetite (Fe3O4@C) nanocomposite [176] to treat simulated hospital effluents (a mixture of 9 antibiotic drugs). The nanocomposite was recyclable, retaining its removal efficiency (up to 85%) after five reutilization cycles. The pH and adsorbent dosage were also adjusted to determine the optimal parameters for effluent treatment.

The adsorption of pharmaceutical pollutants can follow a liquid-film diffusion mechanism, as evidenced by the work of Othman et al. According to the obtained data, the removal of emergent pollutant ketoprofen was achieved using CuNPs [177], which followed a pseudo-first order, exothermic, and supramolecular adsorption. The maximum adsorption of ketoprofen was observed at pH 4.4 based on the pKa of the pollutant drug. The incubation times and adsorbent dosages were also determined (50 min, 1 g/L at room temperature).

Table 8 summarizes the nanomaterials discussed in this section for the remediation of pharmaceutical pollutants.

Table 8. Data on the discussed nanomaterials and nanocomposites for the remediation of pharmaceutical pollutants.

System	Pharmaceutical Pollutant	Maximum RE (%)	Optimal Conditions: pH, Contact Time	Reference
Fe_3O_4@AgNPs	Ibuprofen	93%	pH 7, 45 min.	[170]
Chitosan-Fe_2O_3	Ibuprofen	98%	pH 7, 120 min.	[171]
Starch NPs	Ibuprofen and Sulfamethoxazole	86% (Ibuprofen); 85% (Sulfamethoxazole)	pH 2–3, 300 min.	[172]
Ozone treated MW-CNTs	Acetaminophen	95%	pH 4, 60 min.	[173]
Graphene-TiO_2	Acetaminophen	97%	pH 9, 180 min.	[174]
Maltodextrin-GO-CuO	Diclofenac and Amoxicillin	95%	pH 7, 10 min.	[175]
GO-$CoFe_2O_4$	Diclofenac	87%	pH 4, 120 min.	[176]
Fe_3O_4@C	Hospital effluent (antibiotics)	85%	pH 6, 120 min.	[177]
CuNPs	Ketoprofen	89%	pH 4.4, 50 min	[178]

6. Nanomaterials for the Photodegradation of Pollutants

In addition to detection and remediation methodologies to solve environmental pollution, photodegradation has been developed as a green and economic alternative ascribed to renewable solar energy. Exposure to ultraviolet radiation has been used to degrade toxic pollutants such as agrochemicals, dyes, and organic pollutants, which led to the production of H_2O and the reduction of CO_2 during the degradation process. Further, it has been reported that photocatalytic degradation can be improved by utilizing nanomaterials, nanocomposites, or nanostructures. Nanomaterials for photodegradation must feature an appropriate bandgap (~3 eV), controllable electron-hole recombination rates, electrical conductivity, and corrosion resistance [178–180]. In that regard, photodegradation assisted by semiconductor nanomaterials or nanocomposites is promising because of their charge separation and ability to effectively absorb light in the visible region.

Due to its abundance, low toxicity, and price, TiO_2 has been used as nanoparticles or nanocomposites for photocatalytic degradation. Schwarze et al. [181] reported the immobilization of four commercial TiO_2 onto steel plates for phenol degradation, using H_2O_2 as an oxygen source. Although all the systems proved to be stable, the commercial TiO_2 P90 (crystallite size 13 nm; surface area 103 m^2/g; anatase: rutile composition 87: 13; band gap 3.3 eV) outperformed the rest, with a 100% degradation of phenol within 3 h.

The phenol degradation in seawater was also explored by Xu et al. [182] using two TiO_2-based photocatalysts (Yb-TiO_2-rGO and P25 TiO_2). The photogenerated holes and free radical traps formed in the Yb-TiO2-rGO catalyst featured strong adsorption for phenol compared with the P25-TiO_2 catalyst, in which prominent salt ions in seawater hindered its interaction with phenol. However, treating P25 TiO_2 with ethylene glycol increased the Ti^{3+} content on the catalytic surface, reducing the interference of salt ions.

TiO_2 photocatalytic performance can also be enhanced by embedding nanoparticles on its surface. Jurek et al. prepared a PtNPs/TiO_2 nanocomposite by microemulsion and wet-deposition routes [183]. It was found that the impregnation methods, the chemical state, the morphology, and the size distribution of PtNPs had an impact on the photocatalytic performance of the matrix. The photodegradation studies of phenol confirmed that the SPR of PtNPs initiated the oxidation of the pollutant, which ultimately depended on the morphology of the PtNPs/TiO_2 catalyst.

Although rGO has also been used as a component of nanomaterials for photodegradation applications due to its electronic conductivity and large surface area, the conventional synthesis protocols of rGO are considered not environmentally friendly as they are carried out with hazardous reducing agents. However, new data on greener synthetic approaches have been reported, such as the work by Domínguez et al. rGO was obtained using gobernadora (rGO-GOB) and habanero (rGO-HAB) natural extracts [184]. The photocatalytic performance was evaluated using methylene blue as a pollutant, reaching degradation efficiencies as high as 90%.

WO_3 nanostructures have been formed through anodization and combined with complexing agents to improve photo-electrocatalytic (PEC) properties for the degradation of pollutants. Cifre et al. [185] proposed a WO_3 nanostructure with H_2O_2 and citric acid as complexing agents for the photodegradation of methylparaben. The nanostructure proved to be efficient in removing methylparaben after 4 h. The parameters of the WO_3 synthesis, namely the complexing agents and the annealing temperatures, were also optimized.

Zhou et al. [186] also prepared WO_3 photocatalysts as a strategy for the removal of Rhodamine B under visible light exposure. The WO_3 nanostructure was mixed with Ag_2CO_3 to increase the degradation rate up to 99% within 8 min, 14-fold higher than those of the separate components, as the photo-generated electron-hole pairs in the WO_3/Ag_2CO_3 nanocomposite featured easier separation.

Carbon nitride materials are also proposed for photodegradation applications due to their extended π-conjugated matrix for charge transfer, band gaps of nearly 3 eV, and stability [187].

However, carbon nitride materials are non-metallic, thus exhibiting low conductivity and rapid recombination of electron-hole pairs, hindering their photocatalytic activity. This has led to hybridizing carbon nitride materials with transition metals to improve charge separation and transport properties.

A photocatalyst consisting of SnO_2/C_3N_4 was developed by Singh et al. [188] through wet chemical methods. The synergistic effect of SnO_2/C_3N_4 was evaluated with different mass ratios of each component during the synthesis. The photocatalysts were tested in the degradation of two dyes, Rhodamine-B and Remazol Brilliant-Red, where the highest degradation rates were observed in the 1:1 SnO_2/C_3N_4 nanocomposite.

A similar nanocomposite was fabricated by Mohanta et al. [189] using hydrothermal techniques. The SnO_2/C_3N_4 matrix also incorporated MagNPs to perform LED light-induced photodegradation of carbofuran pollutants while allowing the magnetic separation of the catalyst after its use. The nanocomposite exhibited an efficiency degradation of 89%.

Table 9 summarizes the application of nanomaterials for the photodegradation of pollutants discussed in this section.

Table 9. Results related to the use of nanomaterials and nanocomposites in the photodegradation of pollutants.

System	Pollutant	Degradation (%)	Degradation Time (min)	Reference
TiO_2 P90 on stainless steel	Phenol	100	180	[182]
Yb-TiO_2-rGO	Phenol	100	300	[183]
PtNPs/TiO_2	Phenol	90	30	[184]
rGO-GOB	Methylene Blue	90	120	[185]
rGO-HAB	Methylene Blue	60	120	[186]

Table 9. *Cont.*

System	Pollutant	Degradation (%)	Degradation Time (min)	Reference
WO_3/H_2O_2/citric acid	Methylparaben	100	24 h.	[187]
WO_3/Ag_2CO_3	Rhodamine B	99	8	[188]
SnO_2/C_3N_4	Rhodamine B and Brilliant Red	98	90	[189]
$Fe_3O_4/SnO_2/C_3N_4$	Carbofuran	89	70	[190]

7. Innovative Nanomaterials for Environmental Applications

In addition to the previously described nanomaterials for environmental applications, nanotechnology has also provided solutions in the form of innovative nanomaterials. Functional materials with diverse physicochemical properties for pollutant remediation have been formulated, such as hydrogels, 3D printing at the nanoscale, and nanofibers produced through electrospinning techniques.

Nanometric hydrogels have been used for pollutant removal from wastewater due to their permeability, adsorption capacities, and expandability. Das et al. [190] proposed synthesizing an rGO-chitosan-PVA hydrogel to remove Congo red from the solution. The adsorption capacities of the reinforced hydrogel were tested at different experimental conditions. It was found that the optimal conditions were as follows: pH 2, 140 rpm, and an adsorbent dose of 6 g/L for a removal efficiency of 89%. Further, the presence of rGO on the hydrogel surface increased its thermal stability and porosity.

Salahuddin et al. [191] demonstrated a magnetic hydrogel's effectiveness in removing inorganic pollutants, such as Al, K, Se, Na, V, and S, from a red mud solution. As the MagNPs-hydrogel proved brittle and unstable in compact conditions, cellulose nanofibers (CNFs) were incorporated as a reinforcement agent, and alginate was used as the matrix. The MagNPs-hydrogel-CNFs showed removal efficiencies of over 80% and were retrieved from the solution using a magnet.

Nanotechnology research has also propelled the design of 3D-printed materials for pollutant treatment. The most promising feature of 3D printing is that it allows the design and customization of nanometric adsorbents in terms of their surface areas, stability, morphologies, and thickness [192].

Wang et al. [193] utilized the advantages of 3D printing for the deposition of TiO_2 NPs into a printing resin for the removal of As (III) from wastewater. The 3D printing processes allowed the deposition of the NPs into the 3D resin without compromising their inherent properties. The batch adsorption experiments also demonstrated that the structure could be reutilized up to 10 times and were tested in groundwater samples.

A carbon-ceramic 3D-printed adsorbent was proposed by Figuerola et al. [194] for removing bisphenol A, phenol, ibuprofen, diclofenac, malachite green, and methylene blue from wastewater. Polyvinylidene fluoride was used as a binder and a carbon source for the structure. The manufactured device evidenced removal percentages up to 90% even after ten reutilization cycles. Further, the carbon-ceramic composite was evaluated for the simultaneous extraction of pollutants from tap water samples.

Electrospinning is another versatile technique successfully applied to produce nanomaterials for environmental applications that develops nanofibers through electrostatic repulsion from a viscoelastic fluid. The properties of electro-spun nanofibers feature high porosity and surface areas, thermal stability, and the possibility of being assembled onto other nanostructures [195].

An electro-spun nanofiber for methylene blue removal was designed by Pervez et al. using polyether sulfone and hydroxypropyl cellulose as precursors [196]. The nanofiber exhibited higher mechanical strength, thermal stability, and adsorption capacity than the pristine components. The highest removal efficiency was observed at room temperature at pH 7, exhibiting a reusability of up to five cycles. However, the effect of ionic strength

reduced the adsorption capacity of methylene blue as the metal ions competed for the binding sites on the surface of the nanofiber.

Research conducted by Beiranvand et al. [197] described the synthesis of an electrospun nanofiber based on a graphene/silica composite to remove organic dyes and heavy metals from industrial wastewater.

The composite's thermal, mechanical, and hydrophilic properties were analyzed to confirm their potential applicability as a filter or adsorbent. The obtained data showed removal efficiencies of more than 90%, where the highest adsorption capacities were observed for methylene blue and Pb (II) (>97%) at pH 8 and room temperature. Moreover, the nanofiber showed reusability up to five cycles, retaining a 90% removal efficiency.

8. Nanomaterials: Challenges, and Future Prospects

The emergence of nanomaterials has brought about significant changes in various applications and industries, owing to their distinctive characteristics and properties. Interest in them has been aroused not only for their technological advancements but also within the field of sensor applications, personal care products, textiles, food, medicine, energy, and the removal and degradation of pollutants, among other areas. The extensive range of applications can be attributed to the diverse classifications of nanomaterials, with inorganic, carbon, organic, and composite-based variants being the most prevalent.

Throughout this article, it has been demonstrated that the high surface area generated by these materials enhances sensor responsiveness. This, coupled with a heightened surface contact area with contaminants, facilitates efficient adsorption. Moreover, their photophysical and photochemical properties contribute to the more efficient photodegradation of pollutants, requiring reduced adsorbent quantities.

Notwithstanding their remarkable properties, nanomaterials remain a concern within the scientific community due to uncertainties surrounding their toxicity and potential long-term environmental impact. Although different articles have analyzed the available background information on this [198–200], a comprehensive understanding of nanomaterial toxicity remains to be seen. Divergent results, variations in study conditions, and differences between in vitro and in vivo studies have yet to allow for a clear understanding of the causes of toxicity. Establishing standardized protocols encompassing conditions, concentrations, and cell lines is imperative to delineate the potential adverse effects of nanomaterials.

The practical application of nanomaterials for analytical and environmental purposes encounters significant challenges: first, there is a need to develop procedures to recover and reuse nanomaterials, demonstrating their effectiveness. This focused on the reduction of waste and long-term costs. This approach seeks to foster sustainable analytical and remediation methodologies, accounting for the higher costs associated with these materials; second, the recovery of nanomaterials must align with environmental sustainability goals, emphasizing reusability over disposability; third, assessing the applicability of nanomaterials in real matrices requires in-depth evaluation to explain their diminished analytical response and remediation capacity.

Most of the reported studies primarily focus on laboratory-scale research under controlled conditions. It is necessary to conduct systematic studies of potential species that may interfere with the process and establish specific criteria for the composition of matrices in which the methodology can exhibit better performance. On the other hand, recovering and reusing the material in a natural matrix poses a more significant challenge than laboratory conditions. The interaction of concomitant species with the analyte or contaminant in nanomaterials could hinder the recovery of the material's effectiveness for the intended purposes.

9. Conclusions and Final Remarks

As highlighted and proved in this review, nanomaterials are fascinating interfaces to study, as they present new approaches and possibilities to traditional remediation and detection technologies, as evidenced by their promising removal efficiencies, detection

limits, sensibility, and specificity towards inorganic and organic pollutants. Noble metal nanoparticles, carbon-based nanomaterials, nanocomposites, enzyme-based biosensors, and cyclodextrin derivates were discussed in terms of their unique properties to assess their performance in pollutant remediation and detection, envisioning the possibility of implementing them as an alternative to pollutant treatment in the foreseeable future.

For nanomaterials to be considered sustainable and reliable tools for purification methods, some challenges and future perspectives must be considered, the main one being the limitations of adapting the synthesis of nano-sized technologies to a large-scale production process, facing intense competition from conventional treatment methods. Researchers should not only evaluate the performance of the developed nanomaterials but also consider greener and low-cost approaches for synthesizing them while also investigating their environmental fates to prevent said nanomaterial from becoming a source of contamination. Further, as the efficiency of the nanomaterials is usually studied on a lab scale, evaluating the results under environmental conditions is imperative to ensure their effectual applicability. Nonetheless, nanomaterials will be crucial as future technologies for treating harmful pollutants.

Author Contributions: Conceptualization, S.S.S., T.B., F.M.-B. and P.J.; methodology, S.S.S., T.B., F.M.-B. and P.J.; validation, S.S.S., T.B., F.M.-B., P.J., N.C., C.R.-R., J.G.-C., D.R.G., N.Y., M.U. and A.R.-S.P.; formal analysis, S.S.S., T.B., F.M.-B., P.J., N.C., C.R.-R., J.G.-C., D.R.G., N.Y., M.U. and A.R.-S.P.; investigation, S.S.S., T.B., F.M.-B. and P.J.; resources, T.B., P.J., N.C., C.R.-R., J.G.-C., D.R.G., N.Y., M.U. and A.R.-S.P.; data curation, S.S.S., T.B., F.M.-B. and P.J.; writing—original draft preparation, S.S.S., T.B., F.M.-B., P.J., N.C., C.R.-R., J.G.-C., D.R.G. and A.R.-S.P.; writing—review and editing, S.S.S., T.B., F.M.-B. and P.J.; visualization, S.S.S., T.B., F.M.-B., P.J., N.C., C.R.-R., J.G.-C., D.R.G., N.Y., M.U. and A.R.-S.P.; supervision, S.S.S., T.B., F.M.-B., P.J., N.C., C.R.-R., J.G.-C., D.R.G., N.Y., M.U. and A.R.-S.P.; project administration, T.B., P.J., N.C., C.R.-R., J.G.-C., D.R.G., N.Y., M.U. and A.R.-S.P.; funding acquisition, T.B., P.J., N.C., C.R.-R., J.G.-C., D.R.G., N.Y., M.U. and A.R.-S.P. All authors have read and agreed to the published version of the manuscript.

Funding: This research received no external funding.

Institutional Review Board Statement: Not applicable.

Informed Consent Statement: Not applicable.

Data Availability Statement: Data are contained within the article.

Acknowledgments: The authors would like to acknowledge Proyecto ANID PAI N° 77190012 to Carlos Rojas, Facultad de Ciencias, Universidad de Chile, Proyecto Interno Regular ERP 11500033, and Centro de Investigación Austral Biotech, Universidad Santo Tomás.

Conflicts of Interest: The authors declare no conflict of interest.

Abbreviations

NPs	Nanoparticles
AgNPs	Silver Nanoparticles
AuNPs	Gold Nanoparticles
CuNPs	Copper Nanoparticles
PdNPs	Palladium Nanoparticles
PtNPs	Platinum Nanoparticles
MagNPs	Magnetite Nanoparticles
SPR	Surface Plasmon Resonance
11-MUA	Mercaptoundecanoic acid
BSA	Bovine Serum Albumin
3-MPS	3-mercaptopropyl trimethoxy silane
APD	2-aminopyrimidine-4,6-diol
AMP	Adenosine Monophosphate
TMB	Tetramethylbenzidine
4-MPY	4-mercaptopyridine

PAC	Porous Activated Carbon
GCE	Glassy Carbon Electrode
rGO	Reduced Graphene Oxide
ZnONRs	Zinc Oxide Nanorods
CNTs	Carbon Nanotubes
CNCs	Cellulose Nanocrystals
MOF	Metallic Organic Framework
AChE	Acetylcholinesterase
PYM	Triazine Pymetrozine
SDS	Sodium Dodecyl Sulfate
VNSWCNTs	Nitrogen-Doped Single-Walled Carbon Nanotubes
MW-CNTs	Multi-Walled Carbon Nanotubes
LOD	Limit of Detection
LOQ	Limit of Quantification
DTCs	Dithiocarbamates
MS	Mass Spectrometry
HPLC	High Performance Liquid Chromatography
GC-MS	Gas Chromatography Mass Spectroscopy
LC-MS	Liquid Chromatography Mass Spectroscopy
EIS	Electrochemical Impedance Spectroscopy
CV	Cyclic Voltammetry
DPV	Differential Pulse Voltammetry
DLS	Dynamic Light Scattering
SEM	Scanning Electron Microscopy
TEM	Transmission Electron Microscopy
FT-IR	Fourier Transform Infrared Spectroscopy
XRPD	X-ray Powder Diffraction
EPI	Epichlorohydrin
CDs	Cyclodextrins
NSs	Nanosponges
TPE	Tetrakis (4-hydroxyphenyl) ethene
PMDA	Pyromellitic Dianhydride

References

1. Saravanan, A.; Kumar, P.S.; Jeevanantham, S.; Anubha, M.; Jayashree, S. Degradation of toxic agrochemicals and pharmaceutical pollutants: Effective and alternative approaches toward photocatalysis. *Environ. Pollut.* **2022**, *298*, 118844. [CrossRef]
2. Vardhan, K.H.; Kumar, P.S.; Panda, R.C. A review on heavy metal pollution, toxicity and remedial measures: Current trends and future perspectives. *J. Mol. Liq.* **2019**, *290*, 111197. [CrossRef]
3. Jin, M.; Yuan, H.; Liu, B.; Peng, J.; Xu, L.; Yang, D. Review of the distribution and detection methods of heavy metals in the environment. *Anal. Methods* **2020**, *12*, 5747–5766. [CrossRef]
4. Wagner, M.; Lin, K.Y.A.; Da Oh, W.; Lisak, G. Metal-organic frameworks for pesticidal persistent organic pollutants detection and adsorption—A mini review. *J. Hazard. Mater.* **2021**, *413*, 125325. [CrossRef]
5. Zhang, Y.; Zhu, Y.; Zeng, Z.; Zeng, G.; Xiao, R.; Wang, Y.; Hu, Y.; Tang, L.; Feng, C. Sensors for the environmental pollutant detection: Are we already there? *Coord. Chem. Rev.* **2020**, *431*, 213681. [CrossRef]
6. Wen, N.; Zhang, L.; Jiang, D.; Wu, Z.; Li, B.; Sun, C.; Guo, Z. Emerging flexible sensors based on nanomaterials: Recent status and applications. *J. Mater. Chem. A* **2020**, *8*, 25499–25527. [CrossRef]
7. Karimi-Maleh, H.; Beitollahi, H.; Kumar, P.S.; Tajik, S.; Jahani, P.M.; Karimi, F.; Karaman, C.; Vasseghian, Y.; Baghayeri, M.; Rouhi, J.; et al. Recent advances in carbon nanomaterials-based electrochemical sensors for food azo dyes detection. *Food Chem. Toxicol.* **2022**, *164*, 112961. [CrossRef]
8. Saleh, T.A. Nanomaterials: Classification, properties, and environmental toxicities. *Environ. Technol. Innov.* **2020**, *20*, 101067. [CrossRef]
9. Baig, N.; Kammakakam, I.; Falath, W.; Kammakakam, I. Nanomaterials: A review of synthesis methods, properties, recent progress, and challenges. *Mater. Adv.* **2021**, *2*, 1821–1871. [CrossRef]
10. Ethaib, S.; Al-Qutaifia, S.; Al-Ansari, N.; Zubaidi, S.L. Function of Nanomaterials in Removing Heavy Metals for Water and Wastewater Remediation: A Review. *Environments* **2022**, *9*, 123. [CrossRef]

11. Emenike, E.C.; Iwuozor, K.O.; Anidiobi, S.U. Heavy Metal Pollution in Aquaculture: Sources, Impacts and Mitigation Techniques. *Biol. Trace Element Res.* **2021**, *200*, 4476–4492. [CrossRef]
12. Briffa, J.; Sinagra, E.; Blundell, R. Heavy metal pollution in the environment and their toxicological effects on humans. *Heliyon* **2020**, *6*, e04691. [CrossRef]
13. Bhagat, N.R.; Giri, A. *Nanotechnology for Detection and Removal of Heavy Metals From Contaminated Water*; Wiley: Hoboken, NJ, USA, 2021.
14. Shrivastava, P.; Jain, V.K.; Nagpal, S. Nanoparticle intervention for heavy metal detection: A review. *Environ. Nanotechnol. Monit. Manag.* **2022**, *17*, 100667. [CrossRef]
15. Zamora-Ledezma, C.; Negrete-Bolagay, D.; Figueroa, F.; Zamora-Ledezma, E.; Ni, M.; Alexis, F.; Guerrero, V.H. Heavy metal water pollution: A fresh look about hazards, novel and conventional remediation methods. *Environ. Technol. Innov.* **2021**, *22*, 101504. [CrossRef]
16. Rajendran, S.; Priya, T.; Khoo, K.S.; Hoang, T.K.; Ng, H.-S.; Munawaroh, H.S.H.; Karaman, C.; Orooji, Y.; Show, P.L. A critical review on various remediation approaches for heavy metal contaminants removal from contaminated soils. *Chemosphere* **2021**, *287*, 132369. [CrossRef]
17. Gopinath, K.P.; Madhav, N.V.; Krishnan, A.; Malolan, R.; Rangarajan, G. Present applications of titanium dioxide for the photocatalytic removal of pollutants from water: A review. *J. Environ. Manag.* **2020**, *270*, 110906. [CrossRef]
18. Hosny, M.; Eltaweil, A.S.; Mostafa, M.; El-Badry, Y.A.; Hussein, E.E.; Omer, A.M.; Fawzy, M. Facile Synthesis of Gold Nanoparticles for Anticancer, Antioxidant Applications, and Photocatalytic Degradation of Toxic Organic Pollutants. *ACS Omega* **2022**, *7*, 3121–3133. [CrossRef]
19. Prosposito, P.; Burratti, L.; Venditti, I. Silver nanoparticles as colorimetric sensors for water pollutants. *Chemosensors* **2020**, *8*, 26. [CrossRef]
20. Sultana, K.A.; Islam, M.T.; Silva, J.A.; Turley, R.S.; Hernandez-Viezcas, J.A.; Gardea-Torresdey, J.L.; Noveron, J.C. Sustainable synthesis of zinc oxide nanoparticles for photocatalytic degradation of organic pollutant and generation of hydroxyl radical. *J. Mol. Liq.* **2020**, *307*, 112931. [CrossRef]
21. Alberti, G.; Zanoni, C.; Magnaghi, L.R.; Biesuz, R. Gold and silver nanoparticle-based colorimetric sensors: New trends and applications. *Chemosensors* **2021**, *9*, 305. [CrossRef]
22. Vilela, D.; González, M.C.; Escarpa, A. Sensing colorimetric approaches based on gold and silver nanoparticles aggregation: Chemical creativity behind the assay. A review. *Anal. Chim. Acta* **2012**, *751*, 24–43. [CrossRef]
23. Maghsoudi, A.S.; Hassani, S.; Mirnia, K.; Abdollahi, M. Recent advances in nanotechnology-based biosensors development for detection of arsenic, lead, mercury, and cadmium. *Int. J. Nanomed.* **2021**, *16*, 803–832. [CrossRef]
24. Dong, Y.; Ding, L.; Jin, X.; Zhu, N. Silver nanoparticles capped with chalcon carboxylic acid as a probe for colorimetric determination of cadmium(II). *Microchim. Acta* **2017**, *184*, 3357–3362. [CrossRef]
25. Battocchio, C.; Meneghini, C.; Fratoddi, I.; Venditti, I.; Russo, M.V.; Aquilanti, G.; Maurizio, C.; Bondino, F.; Matassa, R.; Rossi, M.; et al. Silver nanoparticles stabilized with thiols: A close look at the local chemistry and chemical structure. *J. Phys. Chem. C* **2012**, *116*, 19571–19578. [CrossRef]
26. Rossi, A.; Zannotti, M.; Cuccioloni, M.; Minicucci, M.; Petetta, L.; Angeletti, M.; Giovannetti, R. Silver nanoparticle-based sensor for the selective detection of nickel ions. *Nanomaterials* **2021**, *11*, 1733. [CrossRef]
27. Mochi, F.; Burratti, L.; Fratoddi, I.; Venditti, I.; Battocchio, C.; Carlini, L.; Iucci, G.; Casalboni, M.; De Matteis, F.; Casciardi, S.; et al. Plasmonic sensor based on interaction between silver nanoparticles and Ni^{2+} or Co^{2+} in water. *Nanomaterials* **2018**, *8*, 488. [CrossRef]
28. Schiesaro, I.; Burratti, L.; Meneghini, C.; Fratoddi, I.; Prosposito, P.; Lim, J.; Scheu, C.; Venditti, I.; Iucci, G.; Battocchio, C. Hydrophilic Silver Nanoparticles for Hg(II) Detection in Water: Direct Evidence for Mercury-Silver Interaction. *J. Phys. Chem. C* **2020**, *124*, 25975–25983. [CrossRef]
29. Prasad, K.S.; Shruthi, G.; Shivamallu, C. Functionalized silver nano-sensor for colorimetric detection of Hg^{2+} ions: Facile synthesis and docking studies. *Sensors* **2018**, *18*, 2698. [CrossRef]
30. Sharma, P.; Mourya, M.; Choudhary, D.; Goswami, M.; Kundu, I.; Dobhal, M.P.; Tripathi, C.S.P.; Guin, D. Thiol terminated chitosan capped silver nanoparticles for sensitive and selective detection of mercury (II) ions in water. *Sens. Actuators B Chem.* **2018**, *268*, 310–318. [CrossRef]
31. Garg, N.; Bera, S.; Ballal, A. SPR responsive xylenol orange functionalized gold nanoparticles- optical sensor for estimation of Al3+ in water. *Spectrochim. Acta Part A Mol. Biomol. Spectrosc.* **2019**, *228*, 117701. [CrossRef]
32. Sadani, K.; Nag, P.; Mukherji, S. LSPR based optical fiber sensor with chitosan capped gold nanoparticles on BSA for trace detection of Hg (II) in water, soil and food samples. *Biosens. Bioelectron.* **2019**, *134*, 90–96. [CrossRef]
33. Yuan, H.; Ji, W.; Chu, S.; Liu, Q.; Qian, S.; Guang, J.; Wang, J.; Han, X.; Masson, J.-F.; Peng, W. Mercaptopyridine-Functionalized Gold Nanoparticles for Fiber-Optic Surface Plasmon Resonance Hg^{2+} Sensing. *ACS Sens.* **2019**, *4*, 704–710. [CrossRef]
34. Zhu, Y.; Fan, W.; Zhou, T.; Li, X. Removal of chelated heavy metals from aqueous solution: A review of current methods and mechanisms. *Sci. Total Environ.* **2019**, *678*, 253–266. [CrossRef]
35. Feng, J.; Jin, W.; Huang, P.; Wu, F. Highly selective colorimetric detection of Ni^{2+} using silver nanoparticles cofunctionalized with adenosine monophosphate and sodium dodecyl sulfonate. *J. Nanoparticle Res.* **2017**, *19*, 306. [CrossRef]

36. Prosposito, P.; Burratti, L.; Bellingeri, A.; Protano, G.; Faleri, C.; Corsi, I.; Battocchio, C.; Iucci, G.; Tortora, L.; Secchi, V.; et al. Bifunctionalized silver nanoparticles as Hg^{2+} plasmonic sensor in water: Synthesis, characterizations, and ecosafety. *Nanomaterials* **2019**, *9*, 1353. [CrossRef]
37. Prakashan, V.; George, G.; Sanu, M.; Sajna, M.; Saritha, A.; Sudarsanakumar, C.; Biju, P.; Joseph, C.; Unnikrishnan, N. Investigations on SPR induced Cu@Ag core shell doped SiO_2-TiO_2-ZrO_2 fiber optic sensor for mercury detection. *Appl. Surf. Sci.* **2019**, *507*, 144957. [CrossRef]
38. Hutter, E.; Fendler, J.H. Exploitation of localized surface plasmon resonance. *Adv. Mater.* **2004**, *16*, 1685–1706. [CrossRef]
39. Liu, R.; Zuo, L.; Huang, X.; Liu, S.; Yang, G.; Li, S.; Lv, C. Colorimetric determination of lead(II) or mercury(II) based on target induced switching of the enzyme-like activity of metallothionein-stabilized copper nanoclusters. *Microchim. Acta* **2019**, *186*, 250. [CrossRef]
40. Laghari, G.N.; Nafady, A.; Al-Saeedi, S.I.; Sirajuddin; Sherazi, S.T.H.; Nisar, J.; Shah, M.R.; Abro, M.I.; Arain, M.; Bhargava, S.K. Ranolazine-functionalized copper nanoparticles as a colorimetric sensor for trace level detection of as3+. *Nanomaterials* **2019**, *9*, 83. [CrossRef]
41. Yoon, S.J.; Nam, Y.S.; Lee, H.J.; Lee, Y.; Lee, K.B. Colorimetric probe for Ni2+ based on shape transformation of triangular silver nanoprisms upon H2O2 etching. *Sens. Actuators B Chem.* **2019**, *300*, 127045. [CrossRef]
42. Gan, Y.; Liang, T.; Hu, Q.; Zhong, L.; Wang, X.; Wan, H.; Wang, P. In-situ detection of cadmium with aptamer functionalized gold nanoparticles based on smartphone-based colorimetric system. *Talanta* **2020**, *208*, 120231. [CrossRef]
43. Zhang, T.; Jin, H.; Fang, Y.; Guan, J.; Ma, S.; Pan, Y.; Zhu, H.; Liu, X.; Du, M. Detection of trace Cd^{2+}, Pb^{2+} and Cu^{2+} ions via porous activated carbon supported palladium nanoparticles modified electrodes using SWASV. *Mater. Chem. Phys.* **2019**, *225*, 433–442. [CrossRef]
44. Yukird, J.; Kongsittikul, P.; Qin, J.; Chailapakul, O.; Rodthongkum, N. ZnO@graphene nanocomposite modified electrode for sensitive and simultaneous detection of Cd (II) and Pb (II). *Synth. Met.* **2018**, *245*, 251–259. [CrossRef]
45. Hanif, F.; Tahir, A.; Akhtar, M.; Waseem, M.; Haider, S.; Aboud, M.F.A.; Shakir, I.; Imran, M.; Warsi, M.F. Ultra-selective detection of Cd^{2+} and Pb^{2+} using glycine functionalized reduced graphene oxide/polyaniline nanocomposite electrode. *Synth. Met.* **2019**, *257*, 116185. [CrossRef]
46. Hamid, H.A.; Lockman, Z.; Nor, N.M.; Zakaria, N.D.; Razak, K.A. Sensitive detection of Pb ions by square wave anodic stripping voltammetry by using iron oxide nanoparticles decorated zinc oxide nanorods modified electrode. *Mater. Chem. Phys.* **2021**, *273*, 125148. [CrossRef]
47. Giao, N.Q.; Dang, V.H.; Yen, P.T.H.; Phong, P.H.; Ha, V.T.T.; Duy, P.K.; Chung, H. Au nanodendrite incorporated graphite pencil lead as a sensitive and simple electrochemical sensor for simultaneous detection of Pb(II), Cu(II) and Hg(II). *J. Appl. Electrochem.* **2019**, *49*, 839–846. [CrossRef]
48. Sebastian, M.; Aravind, A.; Mathew, B. Green silver-nanoparticle-based dual sensor for toxic Hg(II) ions. *Nanotechnology* **2018**, *29*, 355502. [CrossRef]
49. Sánchez-Calvo, A.; Fernández-Abedul, M.T.; Blanco-López, M.C.; Costa-García, A. Paper-based electrochemical transducer modified with nanomaterials for mercury determination in environmental waters. *Sens. Actuators B Chem.* **2019**, *290*, 87–92. [CrossRef]
50. Bertolacci, L.; Valentini, P.; Pompa, P.P. A nanocomposite hydrogel with catalytic properties for trace-element detection in real-world samples. *Sci. Rep.* **2020**, *10*, 18340. [CrossRef]
51. Kumar, A.; Arya, K.; Mehra, S.; Kumar, A.; Mehta, S.K.; Kataria, R. Detection and sorption of heavy metal ions in aqueous media using Zn-based luminescent metal-organic framework. *Sep. Purif. Technol.* **2023**, *333*, 125875. [CrossRef]
52. Arabbani, F.K.; Vasu, D.; Sakthinathan, S.; Chiu, T.W.; Liu, M.C. A High Efficient Electrocatalytic Activity of Metal-organic Frameworks ZnO/Ag/ZIF-8 Nanocomposite for Electrochemical Detection of Toxic Heavy Metal Ions. *Electroanalysis* **2022**, *35*, e202200284. [CrossRef]
53. Gao, J.; He, D.; Zhang, J.; Sun, B.; Wang, G.; Suo, H.; Zhang, L.; Zhao, C. In-situ growth of porous rod-like tungsten oxide for electrochemical determination of cupric ion. *Anal. Chim. Acta* **2023**, *1276*, 341645. [CrossRef]
54. Radhakrishnan, K.; Sivanesan, S.; Panneerselvam, P. Turn-On fluorescence sensor based detection of heavy metal ion using carbon dots@graphitic-carbon nitride nanocomposite probe. *J. Photochem. Photobiol. A Chem.* **2019**, *389*, 112204. [CrossRef]
55. Bano, S.; Raj, S.I.; Khalilullah, A.; Jaiswal, A.; Uddin, I. Selective and sensitive cation exchange reactions in the aqueous starch capped ZnS nanoparticles with tunable composition, band gap and color for the detection and estimation of Pb^{2+}, Cu^{2+} and Hg^{2+}. *J. Photochem. Photobiol. A Chem.* **2020**, *405*, 112925. [CrossRef]
56. Zeng, H.; Hu, Z.; Peng, C.; Deng, L.; Liu, S. Effective adsorption and sensitive detection of cr(Vi) by chitosan/cellulose nanocrystals grafted with carbon dots composite hydrogel. *Polymers* **2021**, *13*, 3788. [CrossRef]
57. Essiedu, J.A.; Adepoju, F.O.; Ivantsova, M.N. Benefits and limitations in using biopesticides: A review. *AIP Conf. Proc.* **2020**, *2313*, 080002. [CrossRef]
58. Rajmohan, K.S.; Chandrasekaran, R.; Varjani, S. A Review on Occurrence of Pesticides in Environment and Current Technologies for Their Remediation and Management. *Indian J. Microbiol.* **2020**, *60*, 125–138. [CrossRef]
59. Rani, L.; Thapa, K.; Kanojia, N.; Sharma, N.; Singh, S.; Grewal, A.S.; Srivastav, A.L.; Kaushal, J. An extensive review on the consequences of chemical pesticides on human health and environment. *J. Clean. Prod.* **2020**, *283*, 124657. [CrossRef]

60. Tudi, M.; Ruan, H.D.; Wang, L.; Lyu, J.; Sadler, R.; Connell, D.; Chu, C.; Phung, D.T. Agriculture development, pesticide application and its impact on the environment. *Int. J. Environ. Res. Public Health* **2021**, *18*, 1112. [CrossRef]
61. Singh, R.; Kumar, N.; Mehra, R.; Kumar, H.; Singh, V.P. Progress and challenges in the detection of residual pesticides using nanotechnology based colorimetric techniques. *Trends Environ. Anal. Chem.* **2020**, *26*, e00086. [CrossRef]
62. Sharma, P.; Pandey, V.; Sharma, M.M.M.; Patra, A.; Singh, B.; Mehta, S.; Husen, A. A Review on Biosensors and Nanosensors Application in Agroecosystems. *Nanoscale Res. Lett.* **2021**, *16*, 136. [CrossRef]
63. Mirres, A.C.d.M.; Silva, B.E.P.d.M.d.; Tessaro, L.; Galvan, D.; de Andrade, J.C.; Aquino, A.; Joshi, N.; Conte-Junior, C.A. Recent Advances in Nanomaterial-Based Biosensors for Pesticide Detection in Foods. *Biosensors* **2022**, *12*, 572. [CrossRef]
64. Hara, T.O.; Singh, B. Electrochemical Biosensors for Detection of Pesticides and Heavy Metal Toxicants in Water: Recent Trends and Progress. *ACS Environ. Sci. Technol. Water* **2021**, *1*, 462–478. [CrossRef]
65. Kundu, M.; Krishnan, P.; Kotnala, R.K.; Sumana, G. Recent developments in biosensors to combat agricultural challenges and their future prospects. *Trends Food Sci. Technol.* **2019**, *88*, 157–178. [CrossRef]
66. Hazarika, A.; Yadav, M.; Yadav, D.K.; Yadav, H.S. An overview of the role of nanoparticles in sustainable agriculture. *Biocatal. Agric. Biotechnol.* **2022**, *43*, 102399. [CrossRef]
67. Singh, R.P.; Handa, R.; Manchanda, G. Nanoparticles in sustainable agriculture: An emerging opportunity. *J. Control. Release* **2020**, *329*, 1234–1248. [CrossRef]
68. Dimcheva, N. Nanostructures of noble metals as functional materials in biosensors. *Curr. Opin. Electrochem.* **2020**, *19*, 35–41. [CrossRef]
69. Kucherenko, I.S.; Soldatkin, O.O.; Kucherenko, D.Y.; Soldatkina, O.V.; Dzyadevych, S.V. Advances in nanomaterial application in enzyme-based electrochemical biosensors: A review. *Nanoscale Adv.* **2019**, *1*, 4560–4577. [CrossRef]
70. Rajagopalan, V.; Venkataraman, S.; Rajendran, D.S.; Kumar, V.V.; Kumar, V.V.; Rangasamy, G. Acetylcholinesterase biosensors for electrochemical detection of neurotoxic pesticides and acetylcholine neurotransmitter: A literature review. *Environ. Res.* **2023**, *227*, 115724. [CrossRef]
71. Fenoy, G.E.; Marmisollé, W.A.; Azzaroni, O.; Knoll, W. Acetylcholine biosensor based on the electrochemical functionalization of graphene field-effect transistors. *Biosens. Bioelectron.* **2019**, *148*, 111796. [CrossRef]
72. Ajiboye, T.O.; Oladoye, P.O.; Olanrewaju, C.A.; Akinsola, G.O. Organophosphorus pesticides: Impacts, detection and removal strategies. *Environ. Nanotechnol. Monit. Manag.* **2022**, *17*, 100655. [CrossRef]
73. Thakkar, J.B.; Gupta, S.; Prabha, C.R. Acetylcholine esterase enzyme doped multiwalled carbon nanotubes for the detection of organophosphorus pesticide using cyclic voltammetry. *Int. J. Biol. Macromol.* **2019**, *137*, 895–903. [CrossRef]
74. Yi, Y.; Zhou, X.; Liao, D.; Hou, J.; Liu, H.; Zhu, G. High Peroxidase-Mimicking Metal-Organic Frameworks Decorated with Platinum Nanozymes for the Colorimetric Detection of Acetylcholine Chloride and Organophosphorus Pesticides via Enzyme Cascade Reaction. *Inorg. Chem.* **2023**, *62*, 13929–13936. [CrossRef] [PubMed]
75. Han, T.; Wang, G. Peroxidase-like activity of acetylcholine-based colorimetric detection of acetylcholinesterase activity and an organophosphorus inhibitor. *J. Mater. Chem. B* **2018**, *7*, 2613–2618. [CrossRef]
76. El Alami, A.; Lagarde, F.; Huo, Q.; Zheng, T.; Baitoul, M.; Daniel, P. Acetylcholine and acetylcholinesterase inhibitors detection using gold nanoparticles coupled with dynamic light scattering. *Sens. Int.* **2020**, *1*, 100007. [CrossRef]
77. Kong, D.; Jin, R.; Zhao, X.; Li, H.; Yan, X.; Liu, F.; Sun, P.; Gao, Y.; Liang, X.; Lin, Y.; et al. Protein-Inorganic Hybrid Nanoflower-Rooted Agarose Hydrogel Platform for Point-of-Care Detection of Acetylcholine. *ACS Appl. Mater. Interfaces* **2019**, *11*, 11857–11864. [CrossRef] [PubMed]
78. Yu, G.; Wu, W.; Zhao, Q.; Wei, X.; Lu, Q. Efficient immobilization of acetylcholinesterase onto amino functionalized carbon nanotubes for the fabrication of high sensitive organophosphorus pesticides biosensors. *Biosens. Bioelectron.* **2015**, *68*, 288–294. [CrossRef]
79. Du, D.; Wang, M.; Cai, J.; Qin, Y.; Zhang, A. One-step synthesis of multiwalled carbon nanotubes-gold nanocomposites for fabricating amperometric acetylcholinesterase biosensor. *Sens. Actuators B Chem.* **2010**, *143*, 524–529. [CrossRef]
80. Li, H.; Li, F.; Wu, J.; Yang, Q.; Li, Q. Two-dimensional MnO_2 nanozyme-mediated homogeneous electrochemical detection of organophosphate pesticides without the interference of H_2O_2 and color. *Anal. Chem.* **2021**, *93*, 4084–4091. [CrossRef]
81. Wang, S.; Ye, Z.; Wang, X.; Xiao, L. Etching of Single-MnO_2-Coated Gold Nanoparticles for the Colorimetric Detection of Organophosphorus Pesticides. *ACS Appl. Nano Mater.* **2019**, *2*, 6646–6654. [CrossRef]
82. Yan, X.; Kong, D.; Jin, R.; Zhao, X.; Li, H.; Liu, F.; Lin, Y.; Lu, G. Fluorometric and colorimetric analysis of carbamate pesticide via enzyme-triggered decomposition of Gold nanoclusters-anchored MnO_2 nanocomposite. *Sens. Actuators B Chem.* **2019**, *290*, 640–647. [CrossRef]
83. Shu, R.; Wu, Y.; Li, Z.; Zhang, J.; Wan, Z.; Liu, Y.; Zheng, M. Facile synthesis of cobalt-zinc ferrite microspheres decorated nitrogen-doped multi-walled carbon nanotubes hybrid composites with excellent microwave absorption in the X-band. *Compos. Sci. Technol.* **2019**, *184*, 107839. [CrossRef]
84. Kumar, R.; Khan, M.A.; Anupama, A.V.; Krupanidhi, S.B.; Sahoo, B. Infrared photodetectors based on multiwalled carbon nanotubes: Insights into the effect of nitrogen doping. *Appl. Surf. Sci.* **2020**, *538*, 148187. [CrossRef]
85. Li, N.; Shu, R.; Zhang, J.; Wu, Y. Synthesis of ultralight three-dimensional nitrogen-doped reduced graphene oxide/multi-walled carbon nanotubes/zinc ferrite composite aerogel for highly efficient electromagnetic wave absorption. *J. Colloid Interface Sci.* **2021**, *596*, 364–375. [CrossRef] [PubMed]

86. Xu, M.; Jiang, S.; Jiang, B.; Zheng, J. Organophosphorus pesticides detection using acetylcholinesterase biosensor based on gold nanoparticles constructed by electroless plating on vertical nitrogen-doped single-walled carbon nanotubes. *Int. J. Environ. Anal. Chem.* **2019**, *99*, 913–927. [CrossRef]
87. Kumar, T.H.V.; Sundramoorthy, A.K. Electrochemical biosensor for methyl parathion based on single-walled carbon nanotube/glutaraldehyde crosslinked acetylcholinesterase-wrapped bovine serum albumin nanocomposites. *Anal. Chim. Acta* **2019**, *1074*, 131–141. [CrossRef]
88. Zhai, R.; Chen, G.; Liu, G.; Huang, X.; Xu, X.; Li, L.; Zhang, Y.; Wang, J.; Jin, M.; Xu, D.; et al. Enzyme inhibition methods based on Au nanomaterials for rapid detection of organophosphorus pesticides in agricultural and environmental samples: A review. *J. Adv. Res.* **2021**, *37*, 61–74. [CrossRef]
89. Piovesan, J.V.; Haddad, V.F.; Pereira, D.F.; Spinelli, A. Magnetite nanoparticles/chitosan-modified glassy carbon electrode for non-enzymatic detection of the endocrine disruptor parathion by cathodic square-wave voltammetry. *J. Electroanal. Chem.* **2018**, *823*, 617–623. [CrossRef]
90. Ma, L.; He, Y.; Wang, Y.; Wang, Y.; Li, R.; Huang, Z.; Jiang, Y.; Gao, J. Nanocomposites of Pt nanoparticles anchored on UiO66-NH2 as carriers to construct acetylcholinesterase biosensors for organophosphorus pesticide detection. *Electrochim. Acta* **2019**, *318*, 525–533. [CrossRef]
91. Zhang, P.; Sun, T.; Rong, S.; Zeng, D.; Yu, H.; Zhang, Z.; Chang, D.; Pan, H. A sensitive amperometric AChE-biosensor for organophosphate pesticides detection based on conjugated polymer and Ag-rGO-NH2 nanocomposite. *Bioelectrochemistry* **2019**, *127*, 163–170. [CrossRef]
92. Nasiri, M.; Ahmadzadeh, H.; Amiri, A. Organophosphorus pesticides extraction with polyvinyl alcohol coated magnetic graphene oxide particles and analysis by gas chromatography-mass spectrometry: Application to apple juice and environmental water. *Talanta* **2021**, *227*, 122078. [CrossRef]
93. Lazarević-Pašti, T.; Anićijević, V.; Baljozović, M.; Anićijević, D.V.; Gutić, S.; Vasić, V.; Skorodumova, N.V.; Pašti, I.A. The impact of the structure of graphene-based materials on the removal of organophosphorus pesticides from water. *Environ. Sci. Nano* **2018**, *5*, 1482–1494. [CrossRef]
94. Cui, H.F.; Wu, W.W.; Li, M.M.; Song, X.; Lv, Y.; Zhang, T.T. A highly stable acetylcholinesterase biosensor based on chitosan-TiO2-graphene nanocomposites for detection of organophosphate pesticides. *Biosens. Bioelectron.* **2018**, *99*, 223–229. [CrossRef] [PubMed]
95. Dong, P.; Jiang, B.; Zheng, J. A novel acetylcholinesterase biosensor based on gold nanoparticles obtained by electroless plating on three-dimensional graphene for detecting organophosphorus pesticides in water and vegetable samples. *Anal. Methods* **2019**, *11*, 2428–2434. [CrossRef]
96. Ruan, X.; Wang, Y.; Kwon, E.Y.; Wang, L.; Cheng, N.; Niu, X.; Ding, S.; Van Wie, B.J.; Lin, Y.; Du, D. Nanomaterial-enhanced 3D-printed sensor platform for simultaneous detection of atrazine and acetochlor. *Biosens. Bioelectron.* **2021**, *184*, 113238. [CrossRef] [PubMed]
97. Supraja, P.; Tripathy, S.; Vanjari, S.R.K.; Singh, V.; Singh, S.G. Electrospun tin (IV) oxide nanofiber based electrochemical sensor for ultra-sensitive and selective detection of atrazine in water at trace levels. *Biosens. Bioelectron.* **2019**, *141*, 111441. [CrossRef]
98. Ravindran, N.; Kumar, S.; Yashini, M.; Rajeshwari, S.; Mamathi, C.A.; Thirunavookarasu, S.N.; Sunil, C.K. Recent advances in Surface Plasmon Resonance (SPR) biosensors for food analysis: A review. *Crit. Rev. Food Sci. Nutr.* **2021**, *63*, 1055–1077. [CrossRef]
99. Zahran, M.; Khalifa, Z.; Zahran, M.A.H.; Azzem, M.A. Dissolved Organic Matter-Capped Silver Nanoparticles for Electrochemical Aggregation Sensing of Atrazine in Aqueous Systems. *ACS Appl. Nano Mater.* **2020**, *3*, 3868–3875. [CrossRef]
100. Fang, L.; Jia, M.; Zhao, H.; Kang, L.; Shi, L.; Zhou, L.; Kong, W. Molecularly imprinted polymer-based optical sensors for pesticides in foods: Recent advances and future trends. *Trends Food Sci. Technol.* **2021**, *116*, 387–404. [CrossRef]
101. Yılmaz, E.; Özgür, E.; Bereli, N.; Türkmen, D.; Denizli, A. Plastic antibody based surface plasmon resonance nanosensors for selective atrazine detection. *Mater. Sci. Eng. C* **2017**, *73*, 603–610. [CrossRef]
102. Oliveira, T.M.; Ribeiro, F.W.; Sousa, C.P.; Salazar-Banda, G.R.; de Lima-Neto, P.; Correia, A.N.; Morais, S. Current overview and perspectives on carbon-based (bio)sensors for carbamate pesticides electroanalysis. *TrAC Trends Anal. Chem.* **2019**, *124*, 115779. [CrossRef]
103. Moreira, S.; Silva, R.; Carrageta, D.F.; Alves, M.G.; Seco-Rovira, V.; Oliveira, P.F.; Pereira, M.d.L. Carbamate Pesticides: Shedding Light on Their Impact on the Male Reproductive System. *Int. J. Mol. Sci.* **2022**, *23*, 8206. [CrossRef] [PubMed]
104. Öter, Ç.; Zorer, Ö.S. Molecularly imprinted polymer synthesis and selective solid phase extraction applications for the detection of ziram, a dithiocarbamate fungicide. *Chem. Eng. J. Adv.* **2021**, *7*, 100118. [CrossRef]
105. Fanjul-Bolado, P.; Fogel, R.; Limson, J.; Purcarea, C.; Vasilescu, A. Advances in the detection of dithiocarbamate fungicides: Opportunities for biosensors. *Biosensors* **2020**, *11*, 12. [CrossRef] [PubMed]
106. Ghoto, S.A.; Khuhawar, M.Y.; Jahangir, T.M. Silver nanoparticles with sodium dodecyl sulfate as a colorimetric probe for the detection of dithiocarbamate pesticides in environmental samples. *Anal. Sci.* **2019**, *35*, 631–637. [CrossRef] [PubMed]
107. Zúñiga, K.; Rebollar, G.; Avelar, M.; Campos-Terán, J.; Torres, E. Nanomaterial-Based Sensors for the Detection of Glyphosate. *Water* **2022**, *14*, 2436. [CrossRef]
108. Valle, A.L.; Mello, F.C.C.; Alves-Balvedi, R.P.; Rodrigues, L.P.; Goulart, L.R. Glyphosate detection: Methods, needs and challenges. *Environ. Chem. Lett.* **2018**, *17*, 291–317. [CrossRef]

109. Deng, H.-H.; Peng, H.-P.; Huang, K.-Y.; He, S.-B.; Yuan, Q.-F.; Lin, Z.; Chen, R.-T.; Xia, X.-H.; Chen, W. Self-referenced ratiometric detection of sulfatase activity with dual-emissive urease-encapsulated gold nanoclusters. *ACS Sens.* **2019**, *4*, 344–352. [CrossRef]
110. Saenchoopa, A.; Klangphukhiew, S.; Somsub, R.; Talodthaisong, C.; Patramanon, R.; Daduang, J.; Daduang, S.; Kulchat, S. A disposable electrochemical biosensor based on screen-printed carbon electrodes modified with silver nanowires/hpmc/chitosan/urease for the detection of mercury (II) in water. *Biosensors* **2021**, *11*, 351. [CrossRef]
111. Vaghela, C.; Kulkarni, M.; Haram, S.; Aiyer, R.; Karve, M. A novel inhibition based biosensor using urease nanoconjugate entrapped biocomposite membrane for potentiometric glyphosate detection. *Int. J. Biol. Macromol.* **2018**, *108*, 32–40. [CrossRef]
112. Thanh, C.T.; Binh, N.H.; Duoc, P.N.D.; Thu, V.T.; Van Trinh, P.; Anh, N.N.; Van Tu, N.; Tuyen, N.V.; Van Quynh, N.; Tu, V.C.; et al. Electrochemical Sensor Based on Reduced Graphene Oxide/Double-Walled Carbon Nanotubes/Octahedral Fe3O4/Chitosan Composite for Glyphosate Detection. *Bull. Environ. Contam. Toxicol.* **2021**, *106*, 1017–1023. [CrossRef]
113. Byrne, M.P.; Tobin, J.T.; Forrestal, P.J.; Danaher, M.; Nkwonta, C.G.; Richards, K.; Cummins, E.; Hogan, S.A.; O'callaghan, T.F. Urease and nitrification inhibitors-As mitigation tools for greenhouse gas emissions in sustainable dairy systems: A review. *Sustainability* **2020**, *12*, 6018. [CrossRef]
114. Német, N.; Miele, Y.; Shuszter, G.; Tóth, E.L.; Maróti, J.E.; Szabó, P.J.; Rossi, F.; Lagzi, I. Inhibition of the urea-urease reaction by the components of the zeolite imidazole frameworks-8 and the formation of urease-zinc-imidazole hybrid compound. *React. Kinet. Catal. Lett.* **2022**, *135*, 15–28. [CrossRef]
115. Climent, M.J.; Sánchez-Martín, J.; Rodríguez-Cruz, S.; Pedreros, P.; Urrutia, R.; Herrero-Hernández, E. DETERMINATION OF PESTICIDES IN RIVER SURFACE WATERS OF CENTRAL CHILE USING SPE-GC-MS MULTI-RESIDUE METHOD. *J. Chil. Chem. Soc.* **2018**, *63*, 4023–4031. [CrossRef]
116. Sun, M.; Han, S.; Feng, J.; Li, C.; Ji, X.; Feng, J.; Sun, H. Recent Advances of Triazine-Based Materials for Adsorbent Based Extraction Techniques. *Top. Curr. Chem.* **2021**, *379*, 24. [CrossRef]
117. Kang, J.-Y.; Zhang, Y.-J.; Li, X.; Dong, C.; Liu, H.-Y.; Miao, L.-J.; Low, P.J.; Gao, Z.-X.; Hosmane, N.S.; Wu, A.-G. Rapid and sensitive colorimetric sensing of the insecticide pymetrozine using melamine-modified gold nanoparticles. *Anal. Methods* **2017**, *10*, 417–421. [CrossRef]
118. Mangolim, C.S.; Moriwaki, C.; Nogueira, A.C.; Sato, F.; Baesso, M.L.; Neto, A.M.; Matioli, G. Curcumin-β-cyclodextrin inclusion complex: Stability, solubility, characterisation by FT-IR, FT-Raman, X-ray diffraction and photoacoustic spectroscopy, and food application. *Food Chem.* **2014**, *153*, 361–370. [CrossRef] [PubMed]
119. Moradi, S.; Barati, A.; Tonelli, A.E.; Hamedi, H. Chitosan-based hydrogels loading with thyme oil cyclodextrin inclusion compounds: From preparation to characterization. *Eur. Polym. J.* **2019**, *122*, 109303. [CrossRef]
120. Wang, Z.; Zou, W.; Liu, L.; Wang, M.; Li, F.; Shen, W. Characterization and bacteriostatic effects of β-cyclodextrin/quercetin inclusion compound nanofilms prepared by electrospinning. *Food Chem.* **2020**, *338*, 127980. [CrossRef]
121. Liu, Q.; Zhou, Y.; Lu, J.; Zhou, Y. Novel cyclodextrin-based adsorbents for removing pollutants from wastewater: A critical review. *Chemosphere* **2020**, *241*, 125043. [CrossRef]
122. Duan, Z.; Li, Y.; Zhang, M.; Bian, H.; Wang, Y.; Zhu, L.; Xia, D. Towards cleaner wastewater treatment for special removal of cationic organic dye pollutants: A case study on application of supramolecular inclusion technology with β-cyclodextrin derivatives. *J. Clean. Prod.* **2020**, *256*, 120308. [CrossRef]
123. Morin-Crini, N.; Fourmentin, M.; Fourmentin, S.; Torri, G.; Crini, G. Synthesis of silica materials containing cyclodextrin and their applications in wastewater treatment. *Environ. Chem. Lett.* **2018**, *17*, 683–696. [CrossRef]
124. Li, L.; Liu, H.; Li, W.; Liu, K.; Tang, T.; Liu, J.; Jiang, W. One-step synthesis of an environment-friendly cyclodextrin-based nanosponge and its applications for the removal of dyestuff from aqueous solutions. *Res. Chem. Intermed.* **2019**, *46*, 1715–1734. [CrossRef]
125. Iravani, S.; Varma, R.S. Nanosponges for Water Treatment: Progress and Challenges. *Appl. Sci.* **2022**, *12*, 4182. [CrossRef]
126. Krabicová, I.; Appleton, S.L.; Tannous, M.; Hoti, G.; Caldera, F.; Pedrazzo, A.R.; Cecone, C.; Cavalli, R.; Trotta, F. History of cyclodextrin nanosponges. *Polymers* **2020**, *12*, 1122. [CrossRef]
127. Zhen, X.V.; Swanson, E.G.; Nelson, J.T.; Zhang, Y.; Su, Q.; Koester, S.J.; Bühlmann, P. Noncovalent monolayer modification of graphene using pyrene and cyclodextrin receptors for chemical sensing. *ACS Appl. Nano Mater.* **2018**, *1*, 2718–2726. [CrossRef]
128. Verma, M.; Lee, I.; Sharma, S.; Kumar, R.; Kumar, V.; Kim, H. Simultaneous Removal of Heavy Metals and Ciprofloxacin Micropollutants from Wastewater Using Ethylenediaminetetraacetic Acid-Functionalized β-Cyclodextrin-Chitosan Adsorbent. *ACS Omega* **2021**, *6*, 34624–34634. [CrossRef]
129. Zawierucha, I.; Nowik-Zajac, A.; Girek, T.; Lagiewka, J.; Ciesielski, W.; Pawlowska, B.; Biczak, R. Arsenic(V) Removal from Water by Resin Impregnated with Cyclodextrin Ligand. *Processes* **2022**, *10*, 253. [CrossRef]
130. Wang, Z.; Lin, F.; Huang, L.; Chang, Z.; Yang, B.; Liu, S.; Zheng, M.; Lu, Y.; Chen, J. Cyclodextrin functionalized 3D-graphene for the removal of Cr(VI) with the easy and rapid separation strategy. *Environ. Pollut.* **2019**, *254*, 112854. [CrossRef]
131. Lin, S.; Zou, C.; Liang, H.; Peng, H.; Liao, Y. The effective removal of nickel ions from aqueous solution onto magnetic multi-walled carbon nanotubes modified by β-cyclodextrin. *Colloids Surf. A Physicochem. Eng. Asp.* **2021**, *619*, 126544. [CrossRef]
132. Pedrazzo, A.R.; Smarra, A.; Caldera, F.; Musso, G.; Dhakar, N.K.; Cecone, C.; Hamedi, A.; Corsi, I.; Trotta, F. Eco-friendly ß-cyclodextrin and linecaps polymers for the removal of heavy metals. *Polymers* **2019**, *11*, 1658. [CrossRef] [PubMed]

133. Badawi, M.A.; Negm, N.A.; Kana, M.T.H.A.; Hefni, H.H.; Moneem, M.M.A. Adsorption of aluminum and lead from wastewater by chitosan-tannic acid modified biopolymers: Isotherms, kinetics, thermodynamics and process mechanism. *Int. J. Biol. Macromol.* **2017**, *99*, 465–476. [CrossRef] [PubMed]
134. Li, W.; Liu, H.; Li, L.; Liu, K.; Liu, J.; Tang, T.; Jiang, W. Green synthesis of citric acid-crosslinked β-cyclodextrin for highly efficient removal of uranium(VI) from aqueous solution. *J. Radioanal. Nucl. Chem.* **2019**, *322*, 2033–2042. [CrossRef]
135. Cataldo, S.; Meo, P.L.; Conte, P.; Di Vincenzo, A.; Milea, D.; Pettignano, A. Evaluation of adsorption ability of cyclodextrin-calixarene nanosponges towards Pb2+ ion in aqueous solution. *Carbohydr. Polym.* **2021**, *267*, 118151. [CrossRef]
136. Usman, M.; Ahmed, A.; Ji, Z.; Yu, B.; Shen, Y.; Cong, H. Environmentally friendly fabrication of new β-Cyclodextrin/ZrO_2 nanocomposite for simultaneous removal of Pb(II) and BPA from water. *Sci. Total Environ.* **2021**, *784*, 147207. [CrossRef]
137. Rodríguez-López, M.I.; Pellicer, J.A.; Gómez-Morte, T.; Auñón, D.; Gómez-López, V.M.; Yáñez-Gascón, M.J.; Gil-Izquierdo, Á.; Cerón-Carrasco, J.P.; Crini, G.; Núñez-Delicado, E.; et al. Removal of an Azo Dye from Wastewater through the Use of Two Technologies: Magnetic Cyclodextrin Polymers and Pulsed Light. *Int. J. Mol. Sci.* **2022**, *23*, 8406. [CrossRef]
138. Martwong, E.; Chuetor, S.; Junthip, J. Adsorption of Cationic Contaminants by Cyclodextrin Nanosponges Cross-Linked with 1,2,3,4-Butanetetracarboxylic Acid and Poly(vinyl alcohol). *Polymers* **2022**, *14*, 342. [CrossRef]
139. Semeraro, P.; Gabaldón, J.A.; Fini, P.; Núñez-Delicado, E.; Pellicer, J.A.; Rizzi, V.; Cosma, P. Removal of an Azo Textile Dye from Wastewater by Cyclodextrin-Epichlorohydrin Polymers. In *Cyclodextrin—A Versatile Ingredient*; InTech: London, UK, 2018. [CrossRef]
140. Taka, A.L.; Fosso-Kankeu, E.; Pillay, K.; Mbianda, X.Y. Metal nanoparticles decorated phosphorylated carbon nanotube/cyclodextrin nanosponge for trichloroethylene and Congo red dye adsorption from wastewater. *J. Environ. Chem. Eng.* **2019**, *8*, 103602. [CrossRef]
141. Gao, Z.; Li, Y.; Ma, Y.; Ji, W.; Chen, T.; Ma, X.; Xu, H. Functionalized melamine sponge based on β-cyclodextrin-graphene oxide as solid-phase extraction material for rapidly pre-enrichment of malachite green in seafood. *Microchem. J.* **2019**, *150*, 104167. [CrossRef]
142. Kuśmierek, K.; Fronczyk, J.; Świątkowski, A. Adsorptive Removal of Rhodamine B Dye from Aqueous Solutions Using Mineral Materials as Low-Cost Adsorbents. *Water Air Soil Pollut.* **2023**, *234*, 531. [CrossRef]
143. Sulaiman, N.S.; Zaini, M.A.A.; Arsad, A. Evaluation of dyes removal by beta-cyclodextrin adsorbent. *Mater. Today Proc.* **2020**, *39*, 907–910. [CrossRef]
144. Xie, Z.-W.; Lin, J.-C.; Xu, M.-Y.; Wang, H.-Y.; Wu, Y.-X.; He, F.-A.; Jiang, H.-L. Novel Fe3O4Nanoparticle/β-Cyclodextrin-Based Polymer Composites for the Removal of Methylene Blue from Water. *Ind. Eng. Chem. Res.* **2020**, *59*, 12270–12281. [CrossRef]
145. Salazar, S.; Guerra, D.; Yutronic, N.; Jara, P. Removal of aromatic chlorinated pesticides from aqueous solution using β-cyclodextrin polymers decorated with Fe3O4 nanoparticles. *Polymers* **2018**, *10*, 1038. [CrossRef] [PubMed]
146. Salazar, S.; Yutronic, N.; Jara, P. Magnetic β-cyclodextrin nanosponges for potential application in the removal of the neonicotinoid dinotefuran from wastewater. *Int. J. Mol. Sci.* **2020**, *21*, 4079. [CrossRef] [PubMed]
147. Lv, Y.; Ma, J.; Liu, K.; Jiang, Y.; Yang, G.; Liu, Y.; Lin, C.; Ye, X.; Shi, Y.; Liu, M.; et al. Rapid elimination of trace bisphenol pollutants with porous β-cyclodextrin modified cellulose nanofibrous membrane in water: Adsorption behavior and mechanism. *J. Hazard. Mater.* **2020**, *403*, 123666. [CrossRef] [PubMed]
148. Celebioglu, A.; Topuz, F.; Yildiz, Z.I.; Uyar, T. Efficient Removal of Polycyclic Aromatic Hydrocarbons and Heavy Metals from Water by Electrospun Nanofibrous Polycyclodextrin Membranes. *ACS Omega* **2019**, *4*, 7850–7860. [CrossRef] [PubMed]
149. Utzeri, G.; Murtinho, D.; Maria, T.M.; Pais, A.A.C.; Valente, A.J. Amine-β-cyclodextrin-based nanosponges. The role of cyclodextrin amphiphilicity in the imidacloprid uptake. *Colloids Surf. A Physicochem. Eng. Aspects* **2022**, *635*, 128044. [CrossRef]
150. Wang, M.; Li, G.; Xia, C.; Jing, X.; Wang, R.; Liu, Q.; Cai, X. Facile preparation of cyclodextrin polymer materials with rigid spherical structure and flexible network for sorption of organic contaminants in water. *Chem. Eng. J.* **2021**, *411*, 128489. [CrossRef]
151. Demasi, S.; Caser, M.; Caldera, F.; Dhakar, N.K.; Vidotto, F.; Trotta, F.; Scariot, V. Functionalized dextrin-based nanosponges as effective carriers for the herbicide ailanthone. *Ind. Crops Prod.* **2021**, *164*, 113346. [CrossRef]
152. Martwong, E.; Sukhawipat, N.; Junthip, J. Adsorption of Cationic Pollutants from Water by Cotton Rope Coated with Cyclodextrin Polymers. *Polymers* **2022**, *14*, 2312. [CrossRef]
153. Martwong, E.; Sukhawipat, N.; Junthip, J. Cotton Cord Coated with Cyclodextrin Polymers for Paraquat Removal from Water. *Polymers* **2022**, *14*, 2199. [CrossRef]
154. Utzeri, G.; Verissimo, L.; Murtinho, D.; Pais, A.A.C.C.; Perrin, F.X.; Ziarelli, F.; Iordache, T.-V.; Sarbu, A.; Valente, A.J.M. Poly(β-cyclodextrin)-activated carbon gel composites for removal of pesticides from water. *Molecules* **2021**, *26*, 1426. [CrossRef] [PubMed]
155. Koh, E.H.; Moon, J.-Y.; Kim, S.-Y.; Lee, W.-C.; Park, S.-G.; Kim, D.-H.; Jung, H.S. A cyclodextrin-decorated plasmonic gold nanosatellite substrate for selective detection of bipyridylium pesticides. *Analyst* **2020**, *146*, 305–314. [CrossRef] [PubMed]
156. Li, H.; Shi, Y.; Gao, Y. A simple but highly sensitive electropolymerization of L-citrulline and β-cyclodextrin based voltammetric sensor for metribuzin. *Int. J. Environ. Anal. Chem.* **2020**, *102*, 1784–1792. [CrossRef]
157. Tu, X.; Gao, F.; Ma, X.; Zou, J.; Yu, Y.; Li, M.; Qu, F.; Huang, X.; Lu, L. Mxene/carbon nanohorn/β-cyclodextrin-Metal-organic frameworks as high-performance electrochemical sensing platform for sensitive detection of carbendazim pesticide. *J. Hazard. Mater.* **2020**, *396*, 122776. [CrossRef] [PubMed]

158. Danquah, M.K.; Wang, S.; Wang, Q.; Wang, B.; Wilson, L.D. A porous β-cyclodextrin-based terpolymer fluorescence sensor for in situ trinitrophenol detection. *RSC Adv.* **2019**, *9*, 8073–8080. [CrossRef] [PubMed]
159. Alrabiah, H.; Homoda, A.; Bakheit, A.; Mostafa, G.A. Cyclodextrin potentiometric sensors based on selective recognition sites for procainamide: Comparative and theoretical study. *Open Chem.* **2019**, *17*, 1222–1234. [CrossRef]
160. Alrabiah, H.; Aljohar, H.I.; Bakheit, A.H.; Homoda, A.M.A.; Mostafa, G.A.H. Comparative study of β-cyclodextrin, γ-cyclodextrin and 4-tert-butylcalix[8]arene ionophores as electroactive materials for the construction of new sensors for trazodone based on host-guest recognition. *Drug Des. Dev. Ther.* **2019**, *13*, 2283–2293. [CrossRef]
161. Hatami, E.; Ashraf, N.; Arbab-Zavar, M.H. Construction of β-Cyclodextrin-phosphomolybdate grafted polypyrrole composite: Application as a disposable electrochemical sensor for detection of propylparaben. *Microchem. J.* **2021**, *168*, 106451. [CrossRef]
162. Bae, J.; Park, S.J.; Shin, D.-S.; Lee, J.; Park, S.; Kim, H.J.; Kwon, O.S. A Dual Functional Conductive Hydrogel Containing Titania@Polypyrrole-Cyclodextrin Hybrid Nanotubes for Capture and Degradation of Toxic Chemical. *BioChip J.* **2021**, *15*, 162–170. [CrossRef]
163. Nikhil, S.; Karthika, A.; Suresh, P.; Suganthi, A.; Rajarajan, M. A selective and sensitive electrochemical determination of catechol based on reduced graphene oxide decorated β-cyclodextrin nanosheet modified glassy carbon electrode. *Adv. Powder Technol.* **2021**, *32*, 2148–2159. [CrossRef]
164. Feng, G.; Huang, H.; Chen, Y. Effects of emerging pollutants on the occurrence and transfer of antibiotic resistance genes: A review. *J. Hazard. Mater.* **2021**, *420*, 126602. [CrossRef] [PubMed]
165. Khan, N.A.; Khan, S.U.; Ahmed, S.; Farooqi, I.H.; Yousefi, M.; Mohammadi, A.A.; Changani, F. Recent trends in disposal and treatment technologies of emerging-pollutants—A critical review. *TrAC Trends Anal. Chem.* **2019**, *122*, 115744. [CrossRef]
166. Chaukura, N.; Gwenzi, W.; Tavengwa, N.; Manyuchi, M.M. Biosorbents for the removal of synthetic organics and emerging pollutants: Opportunities and challenges for developing countries. *Environ. Dev.* **2016**, *19*, 84–89. [CrossRef]
167. Aguilar-Pérez, K.M.; Avilés-Castrillo, J.I.; Ruiz-Pulido, G. Nano-sorbent materials for pharmaceutical-based wastewater effluents—An overview. *Case Stud. Chem. Environ. Eng.* **2020**, *2*, 100028. [CrossRef]
168. Sigonya, S.; Mokhothu, T.H.; Mokhena, T.C.; Makhanya, T.R. Mitigation of Non-Steroidal Anti-Inflammatory and Antiretroviral Drugs as Environmental Pollutants by Adsorption Using Nanomaterials as Viable Solution—A Critical Review. *Appl. Sci.* **2023**, *13*, 772. [CrossRef]
169. Vicente-Martínez, Y.; Caravaca, M.; Soto-Meca, A.; Solana-González, R. Magnetic core-modified silver nanoparticles for ibuprofen removal: An emerging pollutant in waters. *Sci. Rep.* **2020**, *10*, 18288. [CrossRef]
170. Chahm, T.; Rodrigues, C.A. Removal of ibuprofen from aqueous solutions using O-carboxymethyl-N-laurylchitosan/γ-Fe_2O_3. *Environ. Nanotechnol. Monit. Manag.* **2017**, *7*, 139–148. [CrossRef]
171. Priyan, V.V.; Narayanasamy, S. Effective removal of pharmaceutical contaminants ibuprofen and sulfamethoxazole from water by Corn starch nanoparticles: An ecotoxicological assessment. *Environ. Toxicol. Pharmacol.* **2022**, *94*, 103930. [CrossRef]
172. Yanyan, L.; Kurniawan, T.A.; Albadarin, A.B.; Walker, G. Enhanced removal of acetaminophen from synthetic wastewater using multi-walled carbon nanotubes (MWCNTs) chemically modified with NaOH, HNO3/H2SO4, ozone, and/or chitosan. *J. Mol. Liq.* **2018**, *251*, 369–377. [CrossRef]
173. Tao, H.; Liang, X.; Zhang, Q.; Chang, C.T. Enhanced photoactivity of graphene/titanium dioxide nanotubes for removal of Acetaminophen. *Appl. Surf. Sci.* **2015**, *324*, 258–264. [CrossRef]
174. Moradi, O.; Alizadeh, H.; Sedaghat, S. Removal of pharmaceuticals (diclofenac and amoxicillin) by maltodextrin/reduced graphene and maltodextrin/reduced graphene/copper oxide nanocomposites. *Chemosphere* **2022**, *299*, 134435. [CrossRef]
175. Van Tran, T.; Nguyen, D.T.C.; Le, H.T.N.; Vo, D.V.N.; Nanda, S.; Nguyen, T.D. Optimization, equilibrium, adsorption behavior and role of surface functional groups on graphene oxide-based nanocomposite towards diclofenac drug. *J. Environ. Sci.* **2020**, *93*, 137–150. [CrossRef] [PubMed]
176. Van Tran, T.; Phan, T.-Q.T.; Nguyen, D.T.C.; Nguyen, T.T.; Nguyen, D.H.; Vo, D.-V.N.; Bach, L.G.; Nguyen, T.D. Recyclable Fe3O4@C nanocomposite as potential adsorbent for a wide range of organic dyes and simulated hospital effluents. *Environ. Technol. Innov.* **2020**, *20*, 101122. [CrossRef]
177. ALOthman, Z.A.; Badjah, A.Y.; Alduhaish, O.M.; Rathinam, K.; Panglisch, S.; Ali, I. Synthesis, characterization, kinetics and modeling studies of new generation pollutant ketoprofen removal in water using copper nanoparticles. *J. Mol. Liq.* **2020**, *323*, 115075. [CrossRef]
178. Hu, L.; Ding, Z.; Yan, F.; Li, K.; Feng, L.; Wang, H. Construction of Hexagonal Prism-like Defective BiOCL Hierarchitecture for Photocatalytic Degradation of Tetracycline Hydrochloride. *Nanomaterials* **2022**, *12*, 2700. [CrossRef] [PubMed]
179. Zhang, J.; Chen, X.; Chen, Q.; He, Y.; Pan, M.; Huang, G.; Bi, J. Insights into Photocatalytic Degradation Pathways and Mechanism of Tetracycline by an Efficient Z-Scheme NiFe-LDH/CTF-1 Heterojunction. *Nanomaterials* **2022**, *12*, 4111. [CrossRef]
180. Zang, S.; Cai, X.; Chen, M.; Teng, D.; Jing, F.; Leng, Z.; Zhou, Y.; Lin, F. Tunable Carrier Transfer of Polymeric Carbon Nitride with Charge-Conducting CoV2O6·2H2O for Photocatalytic O2 Evolution. *Nanomaterials* **2022**, *12*, 1931. [CrossRef]
181. Schwarze, M.; Borchardt, S.; Frisch, M.L.; Collis, J.; Walter, C.; Menezes, P.W.; Strasser, P.; Driess, M.; Tasbihi, M. Degradation of Phenol via an Advanced Oxidation Process (AOP) with Immobilized Commercial Titanium Dioxide (TiO_2) Photocatalysts. *Nanomaterials* **2023**, *13*, 1249. [CrossRef]
182. Xu, H.; Hao, Z.; Feng, W.; Wang, T.; Li, Y. Mechanism of Photodegradation of Organic Pollutants in Seawater by TiO_2-Based Photocatalysts and Improvement in Their Performance. *ACS Omega* **2021**, *6*, 30698–30707. [CrossRef]

183. Zielińska-jurek, A.; Wei, Z.; Janczarek, M.; Wysocka, I.; Kowalska, E. Size-controlled synthesis of Pt particles on TiO_2 surface: Physicochemical characteristic and photocatalytic activity. *Catalysts* **2019**, *9*, 940. [CrossRef]
184. Verástegui-Domínguez, L.H.; Elizondo-Villarreal, N.; Martínez-Delgado, D.I.; Gracia-Pinilla, M.Á. Eco-Friendly Reduction of Graphene Oxide by Aqueous Extracts for Photocatalysis Applications. *Nanomaterials* **2022**, *12*, 3882. [CrossRef] [PubMed]
185. Cifre-Herrando, M.; Roselló-Márquez, G.; García-García, D.M.; García-Antón, J. Degradation of Methylparaben Using Optimal WO_3 Nanostructures: Influence of the Annealing Conditions and Complexing Agent. *Nanomaterials* **2022**, *12*, 4286. [CrossRef] [PubMed]
186. Zhou, M.; Tian, X.; Yu, H.; Wang, Z.; Ren, C.; Zhou, L.; Lin, Y.-W.; Dou, L. WO_3/Ag_2CO_3Mixed Photocatalyst with Enhanced Photocatalytic Activity for Organic Dye Degradation. *ACS Omega* **2021**, *6*, 26439–26453. [CrossRef] [PubMed]
187. Prabhu, S.; Pudukudy, M.; Harish, S.; Navaneethan, M.; Sohila, S.; Murugesan, K.; Ramesh, R. Facile construction of djembe-like ZnO and its composite with g-C_3N_4 as a visible-light-driven heterojunction photocatalyst for the degradation of organic dyes. *Mater. Sci. Semicond. Process.* **2019**, *106*, 104754. [CrossRef]
188. Singh, J.; Kumari, P.; Basu, S. Degradation of toxic industrial dyes using SnO_2/g-C_3N_4 nanocomposites: Role of mass ratio on photocatalytic activity. *J. Photochem. Photobiol. A Chem.* **2018**, *371*, 136–143. [CrossRef]
189. Mohanta, D.; Ahmaruzzaman, M. Facile fabrication of novel Fe_3O_4-SnO_2-gC_3N_4 ternary nanocomposites and their photocatalytic properties towards the degradation of carbofuran. *Chemosphere* **2021**, *285*, 131395. [CrossRef]
190. Das, L.; Das, P.; Bhowal, A.; Bhattachariee, C. Synthesis of hybrid hydrogel nano-polymer composite using Graphene oxide, Chitosan and PVA and its application in waste water treatment. *Environ. Technol. Innov.* **2020**, *18*, 100664. [CrossRef]
191. Salahuddin, B.; Aziz, S.; Gao, S.; Hossain, S.A.; Billah, M.; Zhu, Z.; Amiralian, N. Magnetic Hydrogel Composite for Wastewater Treatment. *Polymers* **2022**, *14*, 5074. [CrossRef]
192. Khan, S.B.; Irfan, S.; Lam, S.S.; Sun, X.; Chen, S. 3D printed nanofiltration membrane technology for waste water distillation. *J. Water Process. Eng.* **2022**, *49*, 102958. [CrossRef]
193. Wang, D.; Zhi, T.; Liu, L.; Yan, L.; Yan, W.; Tang, Y.; He, B.; Hu, L.; Jing, C.; Jiang, G. 3D printing of TiO2 nano particles containing macrostructures for As(III) removal in water. *Sci. Total Environ.* **2022**, *815*, 152754. [CrossRef] [PubMed]
194. Figuerola, A.; Rodríguez, F.; Cabello, C.P.; Palomino, G.T. Carbon@ceramic 3D printed devices for bisphenol A and other organic contaminants extraction. *Sep. Purif. Technol.* **2022**, *299*, 121749. [CrossRef]
195. Cui, J.; Li, F.; Wang, Y.; Zhang, Q.; Ma, W.; Huang, C. Electrospun nanofiber membranes for wastewater treatment applications. *Sep. Purif. Technol.* **2020**, *250*, 117116. [CrossRef]
196. Pervez, N.; Talukder, E.; Mishu, M.R.; Buonerba, A.; Del Gaudio, P.; Stylios, G.K.; Hasan, S.W.; Zhao, Y.; Cai, Y.; Figoli, A.; et al. One-Step Fabrication of Novel Polyethersulfone-Based Composite Electrospun Nanofiber Membranes for Food Industry Wastewater Treatment. *Membranes* **2022**, *12*, 413. [CrossRef] [PubMed]
197. Beiranvand, R.; Sarlak, N. Electrospun nanofiber mat of graphene/mesoporous silica composite for wastewater treatment. *Mater. Chem. Phys.* **2023**, *309*, 128311. [CrossRef]
198. Ray, P.C.; Yu, H.; Fu, P.P. Toxicity and environmental risks of nanomaterials: Challenges and future needs. *J. J. Environ. Sci. Health Part C* **2009**, *27*, 1–35. [CrossRef]
199. Zhang, N.; Xiong, G.; Liu, Z. Toxicity of metal-based nanoparticles: Challenges in the nano era. *Front. Bioeng. Biotechnol.* **2022**, *10*, 1001572. [CrossRef]
200. Ganguly, P.; Breen, A.; Pillai, S.C. Toxicity of Nanomaterials: Exposure, Pathways, Assessment, and Recent Advances. *ACS Biomater. Sci. Eng.* **2018**, *4*, 2237–2275. [CrossRef]